CHEMISTRY
A European Journal

A Journal of
ChemPubSoc Europe

Title: A Redox-Switchable Germylene and its Ligating Properties in Selected Transition Metal Complexes

Authors: Florian Walz, Eric Moos, Delphine Garnier, Ralf Köppe, Christopher E. Anson, and Frank Breher

To be cited as: *Chem. Eur. J.* 10.1002/chem.201605073

Link to VoR: http://dx.doi.org/10.1002/chem.201605073

Supported by
ACES

WILEY-VCH

A Redox-Switchable Germylene and its Ligating Properties in Selected Transition Metal Complexes

Florian Walz,[a] Eric Moos,[a] Delphine Garnier,[a,b] Ralf Köppe,[a] Christopher E. Anson,[a]
and Frank Breher[a]*

Abstract: The synthesis, structure, and full characterization of a redox-switchable germylene based on a [3]ferrocenophane ligand arrangement, [Fc(NMes)$_2$Ge] (**4**), is presented. The mesityl (Mes)-substituted title compound is readily available from Fc(NHMes)$_2$ (**2**) and Ge{N(SiMe$_3$)$_2$}$_2$, or from the dilithiated, highly air- and moisture-sensitive compound Fc(NLiMes)$_2$ · 3 Et$_2$O (**3**) and GeCl$_2$. Cyclic voltammetry studies are provided for **4** confirming the above mentioned view of a redox-switchable germylene metalloligand. Although several 1:1 Rh(I) and Ir(I) complexes of **4** (**5** – **7**) are cleanly formed in solution, all attempts to isolate them in pure form failed due to stability problems. However, crystalline solids of [Mo(κ^1*Ge*-**4**)$_2$(CO)$_4$] (**8**) and [W(κ^1*Ge*-**4**)$_2$(CO)$_4$] (**9**) were isolated and fully characterized by common spectroscopic techniques (**8** by X-ray diffraction). DFT calculations were performed on a series of model compounds in order to elucidate a conceivable interplay between the metal atoms in neutral and cationic bimetallic complexes of the type [Rh(κ^1*E*-**qE**)(CO)$_2$Cl]$^{0/+}$ (**qE** = [Fc(NPh)$_2$E] with E = C, Si, Ge). The bonding characteristics of the coordinated Fc-based metalloligands (**qE**/**qE**$^+$) are strongly affected upon *in silico* oxidation of the calculated complexes. The calculated Tolman electronic parameter (TEP) significantly increase by *ca.* 20 cm^{-1} (E = C) to 25 cm^{-1} (E = Si, Ge) upon oxidation. The change in the ligand donating abilities upon oxidation can mainly be attributed to Coulombic effects, while an orbital-based interaction appears to have only a minor influence.

Introduction

In recent years, there has been a growing interest in studying transition-metal complexes based on redox non-innocent ligands.[1] The various types of non-innocent ligands known to date, and the mechanisms through which they influence the reactivity of a metal complex, with a particular attention to the field of catalysis,[2] ion-sensing, or functional molecular materials,[2c,2d,3] for instance, have been summarized in many reviews.

Redox-active ligands offer the possibility to easily modify the electronic properties of a metal complex. As an inherent feature, they carry a fragment capable of gaining or losing electrons, with a concomitant change of the ligation properties, which means that the oxidation/reduction of the ligand affects the Lewis acidity/basicity of both the ligand and coordinated metal center.[4] Furthermore, uncommon reaction paths can be made available by a ligand acting as an electron reservoir.[2c,5] In case the redox-active fragment of the ligand is a metal center, the ligand is frequently referred to as a redox-active metalloligand, that is, a coordination complex as building block in lieu of simple organic ligands.[6] Redox-active ligands of this type usually have a well-defined number of electrons involved in mostly reversible oxidation/reduction processes.

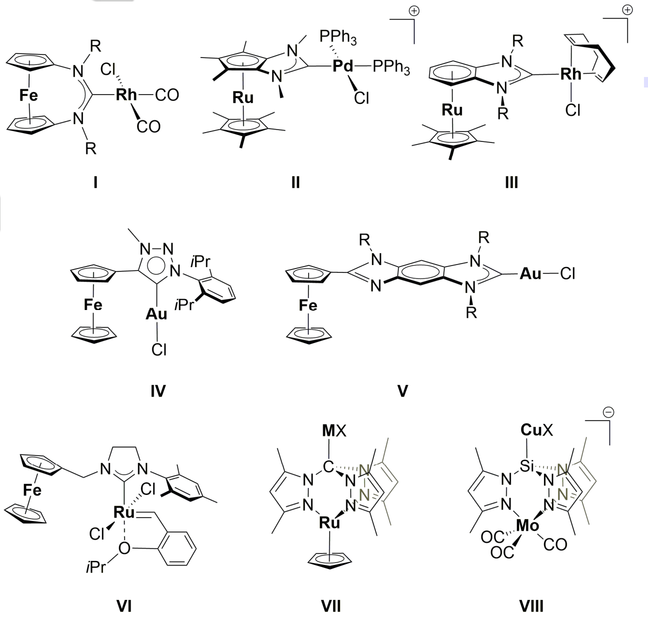

Scheme 1. Selected redox-active metalloligands and their metal complexes (**I**–**VIII**).

Seminal papers reported in this area focused, in particular, on metallocene-based ligand scaffolds, most often containing phosphine-[7] or *N*-donor-based[8] ligand entities attached to the metallocenes. Carbene-based[9] redox-active ligands have also been studied in recent years (Scheme 1).[10] For instance, Siemeling and Bielawski have reported investigations on the

---

[a] Dr. F. Walz, Dr. E. Moos, Dr. D. Garnier, Dr. R. Köppe, Dr. C. E. Anson, Prof. Dr. F. Breher
Institute of Inorganic Chemistry
Karlsruhe Institute of Technology (KIT)
Engesserstr. 15, 76131 Karlsruhe, Germany
E-mail: breher@kit.edu
[b] Dr. D. Garnier (present address)
Institute of Organic Chemistry
University of Stuttgart
Pfaffenwaldring 55, 70569 Stuttgart, Germany

Supporting information for this article is given via a link at the end of the document.

electronic properties and coordination chemistry of NHC derivatives with 1,1'-ferrocenediyl backbones (**I**).[11] Structurally related metal-containing NHC ligands have been published before by Arduengo and co-workers (**II**)[12] and, more recently, by Ganter *et al.* (**III**)[13] NHCs or related derivatives that feature redox-active ferrocenyl substituents and that are ligated to catalytically active metal fragments have recently been applied by the groups of Sarkar (**IV**), Peris (**V**), and Bielawski (**VI**) as redox-switchable catalysts.[14] Somehow related to these redox-active carbene ligands, our research group has investigated the coordination chemistry of Group 14-based tripodal ambidentate ligands,[15] which contain a "free" pyramidal donor site (Scheme 1).[16] For instance, we have recently reported on the synthesis of heterobimetallic complexes containing a redox-switchable, carbanion-based metalloligand (**VII**).[17] In this case, the redox-active, Ru-based ligand is the dominant electron reservoir. Although DFT calculations predicted only marginal changes of the bonding characteristics within the {MX} fragment upon electronic excitation of the ruthenium-based metalloligand, some effect of the influence of {MX} on the $\text{Ru}^{\text{II}}/\text{Ru}^{\text{III}}$ redox potential was detected with the aid of cyclic voltammetry measurements. Related studies have been perfomed for heterobimetallic cuprates consisting of a redox-switchable, silicon-based metalloligand (**VIII**).[18]

The change in the ligand donating abilities upon oxidation of the NHC-derived carbene ligand **FcDAC**[11a] in **I** was found to be largely due to Coulombic effects, where removal of an electron alters the overall molecular charge and increases the Tolman electronic parameter (TEP)[19] by ca. +11 cm^{-1}.[20] In line with this, Ganter and co-workers showed that the inclusion of the unipositive $[\text{RuCp*}]^+$ fragment into the carbene ligand in **III** leads to an experimental ΔTEP of ca. 5 cm^{-1}.[13] In previous studies, however, Wrigthon and co-workers found for ferrocenyl-derived phosphine ligands that both the coordinated and the redox-active metal atom should be arranged in close spatial proximity in order to attain an optimal intermetallic electronic interaction.[21] In this line of thought, Bielawski *et al.* also proposed an orbital-based explanation for the ΔTEP upon oxidation (Scheme 2, top).

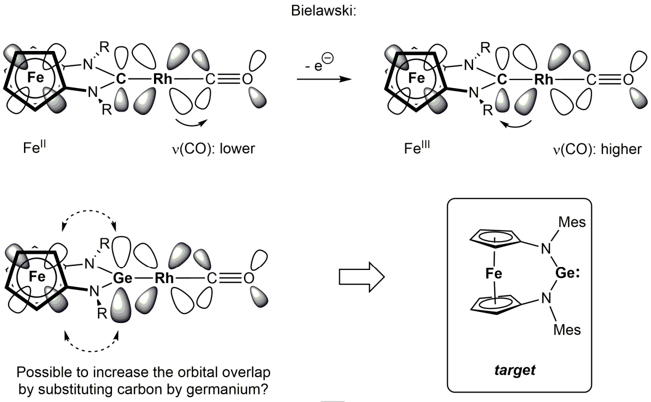

Scheme 2. Top: schematic illustration explaining the effect of oxidizing the FcDAC ligand in **I** (Scheme 1) on the carbonyl stretching frequency (adapted from ref. [11a]); bottom: proposal of this work, replacing C by Ge in order to increase the possible orbital overlap; target molecule of this study. Note that the Rh moiety has been truncated for clarity.

We speculated that the intermetallic communication in these polynuclear scaffolds might be raised by increasing the overall orbital overlap of the constituents. Based on our experience with divalent Group 14 element compounds containing *N*-ligands,[22a-d] and ligands based on heavier group 14 element,[22e-k] we thought to achieve this goal by substituting the carbene C atom in **FcDAC** by a heavier, divalent Group 14 element, *i.e.* by a donor atom featuring much larger and more diffuse valence orbitals, in particular the π-acceptor orbital.[23] Therefore, we became interested in exploring the organometallic and coordination chemistry of heavier analogs of **FcDAC**, in particular a redox-switchable N-heterocyclic germylene (NHGe) based on the [3]ferrocenophane ligand arrangement (target, Scheme 2). Although several germylenes and their transition metal complexes have been reported in recent years,[24] no redox-active version has been published up to date, to the best of our knowledge. Solely Inoue, Enthaler, Dries and co-workers[25] have investigated a 1,1'-ferrocenyl-bridged bis(germylene) featuring amidinate ligands on the Ge atoms, which in turn possess the coordination number 3. In this particular case, however, the Fc entity was introduced as flexible spacer and not for switching purposes.

During the preparation of this manuscript it became apparent that parallel to our studies[26a] the group of Siemeling[26b,27] also prepared differently substituted NHGe (and NHSn) derivatives with the 1,1'-ferrocenediyl backbone, focussing, however, not on their redox-switchable ligating properties but on future investigations on the reactivity of the free, uncoordinated NHGe towards small molecules, also addressing the influence of the redox state.[27] Herein we describe our results on the synthesis, structure and electrochemical properties of the mesityl-substituted diaminogermylene[3]ferrocenophane (**4**) and its first transition metal complexes. Furthermore, quantum chemical calculations on the electronic communication in the heterobimetallic complexes are provided. We are particularly interested in polynuclear complexes of this type in order to explore cooperative effects between metal centers.[28,29]

Results and Discussion

Diaminogermylene[3]ferrocenophane (4)

We initially focused on the mesityl-substituted derivative and used 1,1'-*N*-ferrocenyl diamine ($\text{Fc(NH}_2)_2$, **1**) as starting material.[30] The latter was employed in a literature-known Buchwald-Hartwig coupling reaction with MesBr to provide Fc(NHMes)_2 (**2**) in good yield (Scheme 3).[31] The ^{1}H and ^{13}C NMR spectroscopic data match with those published before by Arnold *et al.*[31] Orange single crystals of **2** suitable for an X-ray diffraction study were grown from Et_2O at -30 °C (space group $P2_1/c$). The molecular structure further confirmed the identity of the product (see Figure S3-1 of the Supporting Information).

Deprotonation of **2** with BuLi in diethyl ether at -78 °C provided the highly air- and moisture-sensitive compound **3** in 41 % isolated yield as an orange, pyrophoric powder, which is only hardly soluble in Et_2O, toluene and benzene (Scheme 3). The absence of an NH stretching band in the IR-ATR spectrum of solid **3** supported the successful dilithiation of the ferrocenyl diamine **2**. The ^{1}H and ^{13}C NMR spectra of **3** in C_6D_6, assigned with the aid of various 2D NMR experiments (^{1}H,^{13}C-*g*HMQC, ^{1}H,^{13}C-*g*HMBC), consist of several sets of signals that are attributed to N(Li)Mes ($\delta_{1\text{H}}$ = 2.09, 2.12, 2.46, 6.91, and 7.23 ppm) and Cp entities ($\delta_{1\text{H}}$ = 2.96, 3.38, 3.54, and 3.73 ppm). It has to be noted, however, that the number of resonances are indicative for an unsymmetrical structure of **3** in solution, in particular if compared with **2** (*cf.*

NHMes: δ_{1H} = 2.12, 2.17, and 6.78 ppm (4.05 ppm for NH); Cp: δ_{1H} = 3.78 and 3.81 ppm; see also Figure S1-1 of the Supporting Information). Integration of the signals revealed that solid **3** contains *ca.* three Et_2O solvent molecules. Note that the dilithiated compound should always be freshly prepared because degradation products can already be detected after some days of storage in an atmosphere of argon. Due to its high sensitivity, no satisfactory elemental analysis could be obtained for **3**.

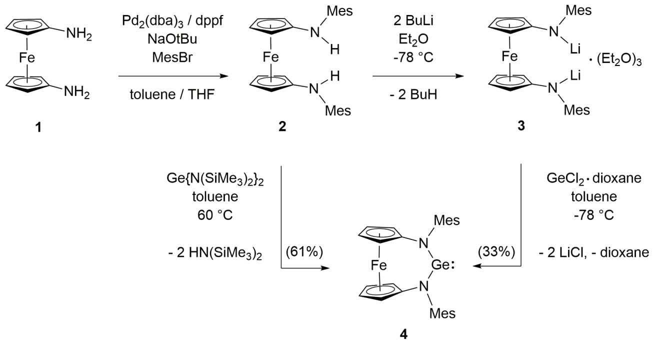

Scheme 3. Synthesis of $[Fc(NMes)_2Ge]$ (**4**).

The target compound $[Fc(NMes)_2Ge]$ (**4**) is accessible *via* two ways, either by reacting the dilithiated **3** with one equivalent of $GeCl_2$·dioxane in toluene at -78 °C and stirring for 15 hours at room temperature (33 % isolated yield after work-up) or by treating one equivalent of $Ge\{N(SiMe_3)_2\}_2$[32] with **2** in toluene at 60 °C. Although the isolated yield of **4** is significantly higher in this case (61 %), the reaction time is considerably longer (2 weeks). **4** is very soluble in toluene, benzene and tetrahydrofurane; acetonitrile was found to react with the germylene under formation of **2**. Compound **4** is a (very) moisture and air-sensitive red solid that is thermally stable (m.p. = 235-237 °C). Their UV/Vis spectrum in THF shows broad bands around λ = 456 (ε = 962 $dm^3mol^{-1}cm^{-1}$) and 294 nm (ε = 16360 $dm^3mol^{-1}cm^{-1}$), which correspond to ferrocene-based *d*–*d* transitions[33] and fall in the typical range found for 1,1'-ferrocene diamines.[34]

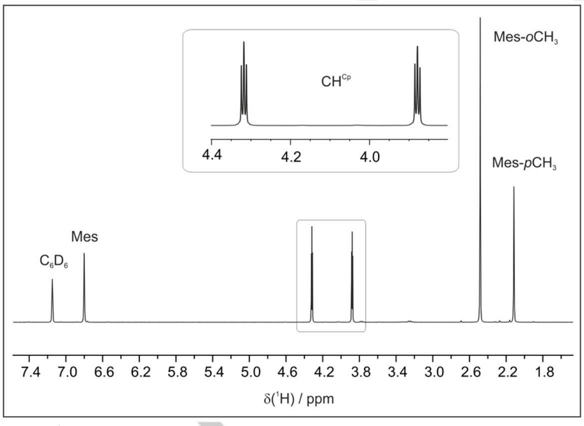

Figure 1. ^1H NMR spectrum of **4** in C_6D_6 at room temperature. The inset is showing the region of the CH^{Cp} signals.

Contrary to **3**, the ^1H and ^{13}C NMR spectra of **4** in C_6D_6 consist of simple sets of signals that are attributed to the mesityl and cyclopentadienyl entities. The ^1H NMR spectrum exhibits two signals corresponding to the methyl group of the Mes ligands in the ortho- and para-positions at δ_{1H} = 2.49 and 2.13 ppm, respectively, while the respective signals for the aromatic CH^{Mes} group appears at 6.81 ppm. The signal for the CH^{Cp} entities were detected as two well-separated pseudo-triplets (AA'BB' spin system; for a simulation of the spectrum, see Figure S1-2 of the Supporting Information) with chemical shifts of δ = 3.89 and 4.33 ppm (Figure 1). The rather simple, symmetric structure of **4** in solution was also confirmed by ^{13}C NMR spectroscopy (see Experimental Part for details).

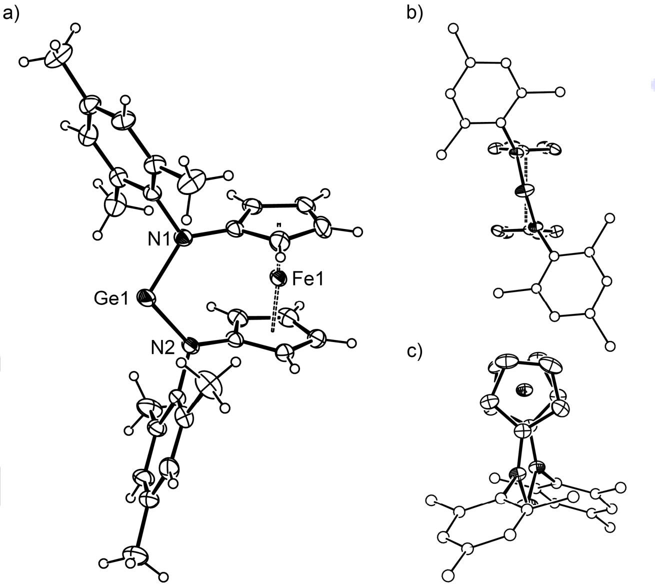

Figure 2. Molecular structure of **4** (a, displacement ellipsoids are drawn at the 30% probability level) and different top and side views (b and c). Selected bond lengths and distances (pm) and angles (°): Fe1–C1 201.35(16), Fe1–C2 202.53(19), Fe1–C3 204.05(19), Fe1–C4 206.4(2), Fe1–C5 203.63(18), Fe1–C6 201.68(16), Fe1–C7 203.60(18), Fe1–C8 205.49(18), Fe1–C9 203.93(19), Fe1–C10 202.48(17), Fe1–Cp_{cent}(1) 163.9, Fe1–$Cp_{cent(2)}$ 163.7, Ge1–N1 184.59(14), Ge1–N2 184.43(14), Ge1...Fe1 381.7, N1–C1 141.6(2), N2–C6 141.3(2), N1–C11 143.9(2), N2–C20 144.3(2); N1–Ge1–N2 103.67(6), Ge1–N1–C1 131.10(11), Ge1–N2–C6 130.53(11), C1–Fe1–C6 100.70(7), C3–Fe1–C8 113.24(9), C4–Fe1–C9 112.98(9). (Cp_{cent} = centroids of the Cp rings)

Crystals of $[Fc(NMes)_2Ge]$ (**4**) suitable for X-ray crystallography were obtained from a concentrated Et_2O solution at -40 °C (Figure 2; space group $P2_1/c$). As expected, the germanium center in **4** is bonded to two NMes entities (∠N1–Ge1–N2 = 103.67°). The bridging of the 1,1'-*N*-ferrocenyldi(mesitylamido) scaffold by the germanium(II) atom results in slightly inclined Cp rings, which can be seen from the ca. 10 pm shorter iron–carbon bond lengths Fe1–C1 (201.35 pm) and Fe1–C6 (201.68 pm) as compared to those observed for **3** (see the Supporting Information). Nevertheless, the ferrocene entity adopts an S-1,1'-synclinic conformation (Figure 2b). The carbon–nitrogen bond lengths C1–N1 and C6–N2 of 141.6 and 141.3 pm, respectively, are ca. 3 pm longer than in **3**. The Ge–N distances of 184.59 and 184.43 pm fall in the typical range found for other five- and six-membered *N*-heterocyclic germylenes (NHGe).[35] NHGes based on β-diketiminates or amidinates and halogermylenes derived from 1,3-diazaindanes usually show longer Ge–N distances.[36]

Since we intended to employ **4** as redox-switchable ligand in coordination chemistry, we became interested in quantifying its size. To this end, we have calculated the buried volume (%V_{bur})[37] on the basis of the molecular structure. The %V_{bur} value of 39.2 (d = 200 pm; r = 350.0 pm)[38] reasonably compares with those obtained for the Fc-based NHC derivatives **V1**, **V4** and **V5** (Scheme 4) but is somewhat larger than those published for purely organic N-heterocyclic carbenes (**V6-V8**) or the derivatives **V2** and **V3** featuring smaller substituents on nitrogen.[39]

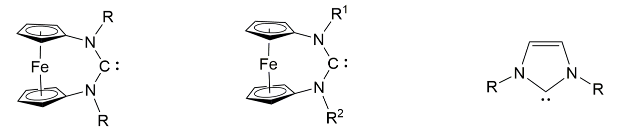

V1 (R = Ad): 39.3[a]
V2 (R = *i*Bu): 27.3[b]
V3 (R = Np): 30.6[a]

V4 (R^1 = Np, R^2 = Anth): 34.9[a]
V5 (R^1 = Np, R^2 = Ad): 36.2[a]

V6 (R = Cy): 27.3-27.6[c]
V7 (R = Mes): 33.0-33.8[c]
V8 (R = Dipp): 34.0-34.9[c]

Scheme 4. %V_{bur} values (d = 200 pm; r = 350.0 pm) of some selected compounds. [a] calculated from the molecular structure of the Rh(cod)Cl complex;[11] [b] calculated from the molecular structure of the $Ir(CO)_2Cl$ complex;[11] [c] taken from the literature (based on Rh(I) and Ir(I) complexes).[39b]

Cyclic voltammetry studies on **4** were conducted in THF at room temperature. Although the THF/[nBu$_4$N][Al{OC(CF$_3$)$_3$}$_4$] electrolyte was stored over sodium and thoroughly dried glassware was used in a special setup for inert conditions developed by Heinze,[40] **4** is rapidly hydrolyzed by trace amounts of water to the parent amine **2** (Figure 3). The latter shows a quasi-reversible redox process centered at $E^0{}_{1/2}$ = -0.69 V (vs. the ferrocene/ferrocenium couple, Fc/Fc$^+$), which perfectly fits to studies reported previously by Diaconescu[34] and Siemeling.[27] The quasi-reversible oxidation of **4** detected at $E^0{}_{1/2} \cong 0.15$ V is slightly more anodically shifted as compared to the value reported by Siemeling and co-workers ($E^0{}_{1/2}$ = -0.055 V),[27] which may be be attributed to differences in the experimental conditions or artefacts resulting from the relatively large ΔE^p value of ca. 400 mV observed in our case. Note that the very limited publications on the electrochemistry of NHGe derivatives only report irreversible oxidation processes in THF at $E^p{}_a \cong 0.48$ and 0.85 V (vs. Fc/Fc$^+$),[41] *i.e.* at much higher potentials. Quantum chemical calculations performed by us (*vide supra*) and Siemelig *et al.*[27] clearly showed that the spin density in the cationic complex, *i.e.* **4$^+$**, is largely located on the Fe atom of the ferrocenyl-backbone. Attempts to prepare **4$^+$** on a preparative scale have not yet been successful but are still in the current focus of interest.

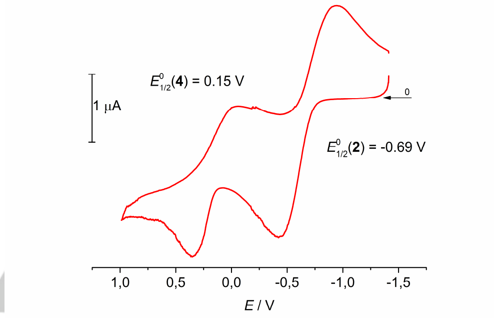

Figure 3. Cyclic voltammogram of **4** in THF at r.t. *vs.* the Fc/Fc$^+$ couple; Scan rate 250 mV s^{-1}, Pt/[nBu$_4$N][Al{OC(CF$_3$)$_3$}$_4$]/Ag.

Metal complexes of 4

Previous investigations on **FcDAC**-type carbene ligands have revealed that such species can act as κ^1C ligands. Therefore, we became interested in studying the coordination behavior of the heavy analog **4** as well. ^{1}H NMR spectroscopic monitoring of the reaction of two equivs. of **4** with one equiv. of the dimers [Rh(cod)Cl]$_2$ and [Ir(cod)Cl]$_2$ in C_6D_6 or d$_8$-thf provided evidence for the formation of [Rh(κ^1*Ge*-**4**)(cod)Cl] (**5**) and [Ir(κ^1*Ge*-**4**)(cod)Cl] (**6**) (Scheme 5, Figure 4). Typical signal patterns for 1:1 complexes of **4** with Rh or Ir are observed (see Experimental Part for details). The numbers of ^{1}H and ^{13}C NMR signals suggest rather symmetrical structures in solution, which may be a result of rapidly rotating metal and germylene entities around the Ge-M bond on the NMR time scale. Pulsed gradient spin-echo (PGSE) experiments were performed in d$_8$-thf. The hydrodynamic radii (r_H(**5**)= 4.80 Å, r_H(**6**)= 5.28 Å) and volumes (V_H(**5**) = 463 Å^3, V_H(**6**) = 616 Å^3) in d$_8$-thf solution were obtained by using the experimental self-diffusion coefficients (D(**5**) = $9.775 \cdot 10^{-10}$ m^2 s^{-1}, D(**6**) = $8.888 \cdot 10^{-10}$ m^2 s^{-1}) together with the Stokes-Einstein equation. Note that both V_H values for the complexes are very close to the volume for an individual molecule of the free germylene (**4**) estimated from X-ray crystallographic studies ($V_{X\text{-}ray}$ = 610 Å^3). However, close inspection of the diffusion properties of, *e.g.*, the Cp proton signals of the germylene unit and the cod signals of the [M(cod)Cl] entities verified very similar results (see Section S1 of the Supporting Information). Based on these data it seems reasonable to assume that **4** indeed forms 1:1 complexes with [M(cod)Cl]. However, all attempts to isolate **5** and **6** in pure form failed. Only decomposition products have been obtained so far.

In order to further substantiate the formation of the Rh(I) and Ir(I) complexes **5** and **6**, respectively, we have treated a solution of **6** with CO gas (p = *ca.* 1 bar) (Scheme 5, Figure 5). The signals for free 1,5-cyclooctadiene (cod) are immediately visible in the ^{1}H NMR spectrum (Figure 5). As compared to **6**, the number of ^{1}H and ^{13}C NMR signals observed for [Ir(κ^1*Ge*-**4**)(CO)$_2$Cl] (**7**) doubles which would be in accordance with a lower symmetry of **7**. For instance, the *ortho*-methyl protons of the Mes substituents gave two signals with chemical shifts of δ_{1H} = 2.56 and 2.64 ppm and four ^{1}H NMR signals are detected for the Cp protons (Figure 5). As expected, two resonances are found in the ^{13}C{^{1}H} NMR spectrum for two different CO ligands (δ_{13C} = 166.0 and 185.2 ppm; Figure 5). Albeit its clean and almost quantitative formation in solution, all attempts to isolate **7** from the reaction mixtures failed so far.

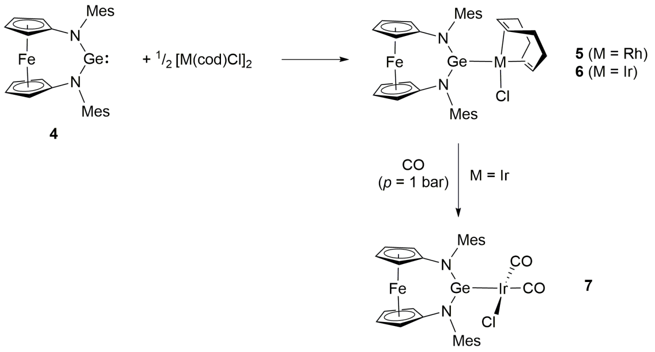

Scheme 5. Synthesis of [Rh(κ^1*Ge*-**4**)(cod)Cl] (**5**), [Ir(κ^1*Ge*-**4**)(cod)Cl] (**6**), and [Ir(κ^1*Ge*-**4**)(CO)$_2$Cl] (**7**). Note that all complexes have only been observed in solution and decompose upon attempted isolation.

More successful attempts to isolate a metal complex of **4** have been made by treating the germylene with the hexacarbonyls of molybdenum and tungsten under irradiation for 2 h in tetrahydrofuran (Scheme 6). Layering of the reaction solutions with pentane or hexane furnished bright orange, crystalline solids of [Mo(κ^1*Ge*-**4**)$_2$(CO)$_4$] (**8**) and [W(κ^1*Ge*-**4**)$_2$(CO)$_4$] (**9**) in 49 % and 14 % isolated yields, respectively. We were not able to detect or isolate any hypothetical 1:1 metal-ligand complexes of the general formula [M(κ^1*Ge*-**4**)(CO)$_5$], which may be a result of the *trans*-effect exerted by **4**.[42]

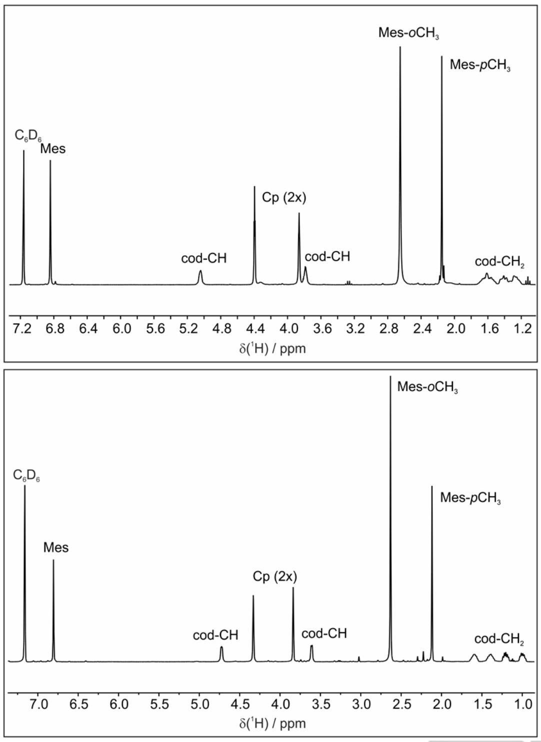

Figure 4. ^{1}H NMR spectra of [Rh(κ^1*Ge*-**4**)(cod)Cl] (**5**, top) and [Ir(κ^1*Ge*-**4**)(cod)Cl] (**6**, bottom) in C_6D_6 at room temperature.

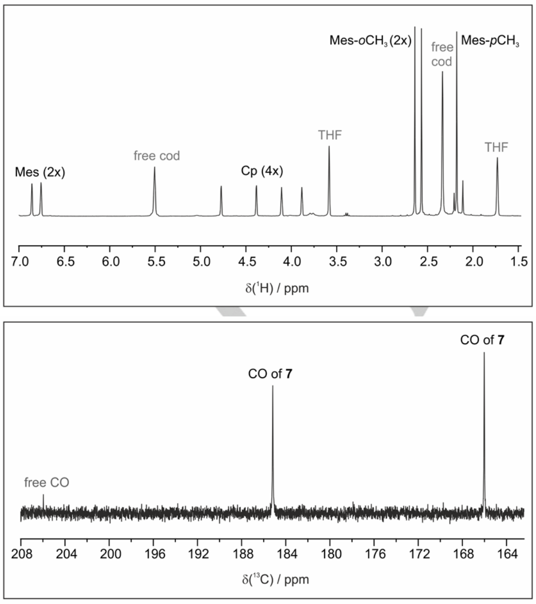

Figure 5. ^{1}H NMR spectrum (top) and section of the ^{13}C NMR spectrum (bottom) of [Ir(κ^1*Ge*-**4**)(CO)$_2$Cl] (**7**) in C_6D_6 at room temperature.

Both complexes are sparingly soluble in hexane or pentane, but show a good solubility in toluene, benzene, and THF, and are thermally stable with decomposition points > 230 °C. The NMR spectra of the complexes are consistent with the formation of symmetrical 1:2 metal-ligand species in all cases (Figure 6). For instance, only one ^{13}C NMR signal was detected for the CO ligands at δ_{13C} = 207.7 (**8**) and 197.7 (**9**) ppm. The signals fall in the expected range found for other 1:2 molybdenum or tungsten germylene complexes in the literature.[43]

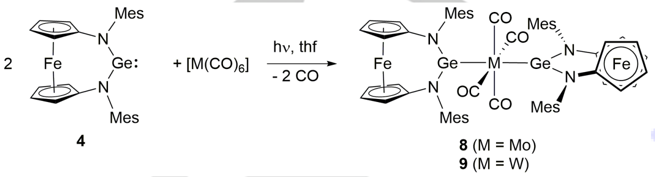

Scheme 6. Synthesis of [Mo(κ^1*Ge*-**4**)$_2$(CO)$_4$] (**8**) and [W(κ^1*Ge*-**4**)$_2$(CO)$_4$] (**9**).

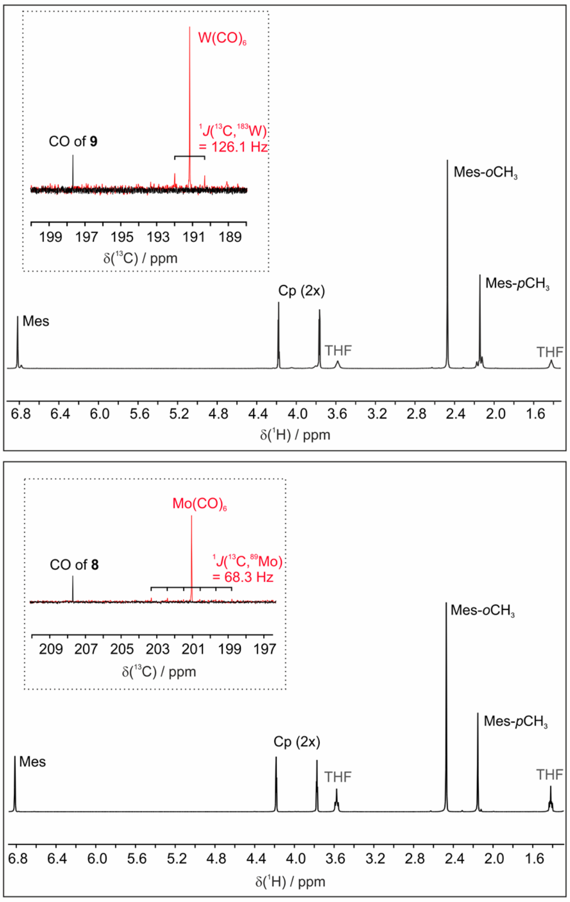

Figure 6. ^{1}H NMR spectrum of [Mo(κ^1*Ge*-**4**)$_2$(CO)$_4$] (**8**, bottom) and [W(κ^1*Ge*-**4**)$_2$(CO)$_4$] (**9**, top) in C_6D_6 at room temperature. Insets are showing sections of the ^{13}C NMR spectra, also overlaid with the ^{13}C NMR spectrum of the starting mateials [W(CO)$_6$] and [Mo(CO)$_6$].

Further evidence for the formation of 1:2 (instead of 1:1) complexes was provided by IR and Raman investigations (Figure 7). Both complexes show a strong CO band at ν^{IR}(**8**) = 1916 and ν^{IR}(**9**) = 1905 cm^{-1}. Additional Raman investigations on **8** provided two bands at ν^{RA}(**8**) = 1971 and 2038 cm^{-1} (**9** decomposes under

10.1002/chem.201605073

laser irradiation). The spectral data gave clear evidence of a local D_{4h} symmetry around the metal atom and, thus, one IR-active (E_u) and two Raman-active (A_{1g} and B_{2g}) CO stretches. Note that compared to NHGe molybdenum complexes of the net formula [$L_3Mo(CO)_3$] (L = NHGe), the CO band of **8**, provided by the IR investigation, was detected at lower frequencies (60-45 cm^{-1} less).[45]

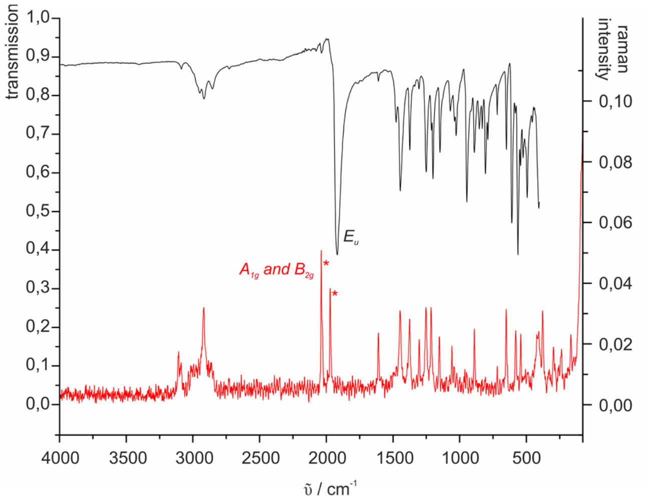

Figure 7. FT-IR (black) and Raman spectrum (red) of solid [Mo(κ^1*Ge*-**4**)$_2$(CO)$_4$] (**8**).

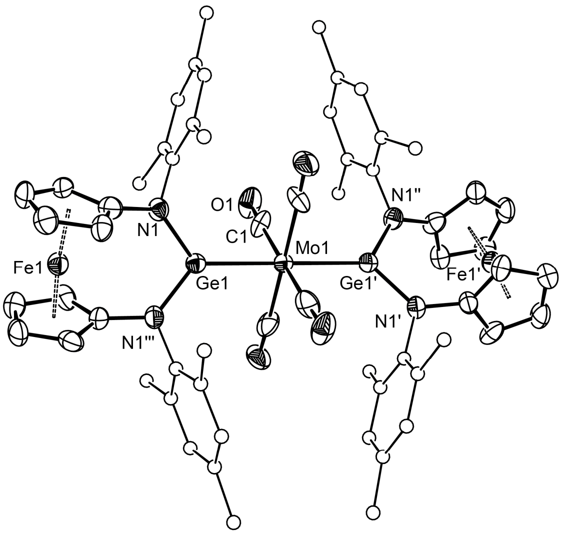

Figure 8. Molecular structure of [Mo(κ^1*Ge*-**4**)$_2$(CO)$_4$] (**8**). Displacement ellipsoids are drawn at the 30% probability level, carbon atoms of the Mes ligands as spheres, for clarity reasons. Selected bond lengths (pm) and angles (°): Ge1–Mo1 249.40(16), Mo1–C1 203.4(15), C1–O1 111.3(16), Ge1–N1 181.0(11), Ge1···Fe1 377.1, N1–C2 143.7(18), N1–C7 149.6(17), Fe1–C2 198.7(15), Fe1–C3 203.0(13), Fe1–C4 204.3(18), Fe1–C5 203.5(17), Fe1–C6 202.5(14), Fe1–Cp$_{cent}$(1) 162.7; O1–C1–Mo1 178.8(15), C1–Mo1–C1’ 178.6(16), C1–Mo1–C1’’ 91.9(8), C1–Mo1–C1’’’ 88.2(8), C1’–Mo1–C1’’’ 89.3(8), C1’’–Mo1–C1’’’ 90.7(8), Ge1–Mo1–C1 90.7(8), Ge1–Mo1–C1’’ 89.3(8), Ge1–Mo1–Ge1’ 180.0, N1–Ge1–Mo1 127.6(4), N1–Ge1–N1’’’ 104.8(7), Ge1–N1–C2 128.9(10), Ge1–N1–C7 119.7(9), C2–N1–C7 111.2(11), C2–Fe1–C2’’’ 100.7(9), C3–Fe1–C3’’’ 166.4(8), C4–Fe1–C4’’’ 124.0(9), C5–Fe1–C5’’’ 137.5(9), C6–Fe1–C6’’’ 141.6(8). (Cp$_{cent}$ = centroid of the Cp ligand). Atoms labeled with apostrophes are generated by –x+1, -y+1, z ('), y, x, -z+1 ("), and –y+1, -x+1, -z+1 (''').

Crystals of **8** suitable for X-ray crystallography were obtained by layering a concentrated THF solution with hexane (Figure 8; space group $P4_22_12$) and the crystallographic analyses unambiguously confirm the 1:2 structures suggested by the spectroscopic evidence.

The Mo center in **8** is coordinated by two germylene entities in *trans*-position and four CO ligands. All structural parameters are in good agreement with those observed for another 1:2 molybdenum complexes of a halogermylene.[43b] We are not aware of any other reports on 1:2 molybdenum complexes of germylenes featuring this *trans* arrangement. The Ge-Mo bond length (249.40 pm) is very similar to the closely related 1:2 molybdenum complex of a halogermylene (249.90 pm).[43b] Slightly longer Ge-Mo bond length were observed for five-membered *N*-heterocyclic germylene complexes ([$L_3Mo(CO)_3$], L = NHGe) (252.85, 254.45, 254.52 pm)[44a,b] and a chelate complex featuring a bis(germylene) ([$L_2Mo(CO)_4$], L = NHGe) (252.04 pm).[44c] The Ge-N bond length (181.0) pm) is marginally shorter than those observed in **4** (184.59, 184.43 pm), *i.e.* the free germylene.

Cyclic voltammetry studies on **8** and **9** in THF at room temperature showed that also the coordination compounds of Fc(NMes)$_2$Ge are extremely sensitive to moisture. Nevertheless, apart from the typical redox process for the product of hydrolysis, i.e. the amine **2**, quasi reversible redox waves were detected at $E^0_{1/2}$(**8**) = -0.03 V and $E^0_{1/2}$(**9**) = -0.02 V (vs. Fc/Fc$^+$) with peak potential differences of ΔE^p(**8**) = 115 mV and ΔE^p(**9**) = 91 mV, respectively (See section S2 of the Supporting Information). From these values it can be concluded that the redox potential of the Fc-based NHGe (**4**) is only slightly affected upon coordination. Furthermore, it has to be noted that we did not detect a conceivable splitting of the half-wave potentials due to metal-to-metal communcation between both ferrocenyl entities in the κ^1*Ge*-coordinated germylenes in **8** and **9**.[45]

Quantum Chemical Calculations

In order to elucidate a conceivable interplay between the metal atoms in the bimetallic complexes, we initially focused on a change of the bonding characteristics of the redox-switchable germylene **4** upon oxidation. To this end, we have performed some density functional theory (DFT) computations with the Turbomole program package. We have chosen **qGe** as model compound of **4** for this study containing phenyl instead of mesityl substituents on nitrogen (Figure 9) and used the def2-TZVP basis sets (see Experimental Part for details).

Table 1. Selected geometry parameters (bond lengths in pm, angles in °) of the model compounds **qE/qE⁺** with E = C, Si, Ge.

Compound	avg. Fe-C	avg. E-N	N-E-N	Fe···E
4 (XRD)[a]	202.8	183.9	103.7	381.7
qGe	206.5	191.0	104.0	380.4
qGe⁺	212.2	192.6	100.9	387.8
qSi	206.2	177.2	107.2	374.5
qSi⁺	211.5	177.6	104.9	380.6
qC	205.4	135.1	122.3	341.2
qC⁺	210.8	135.1	122.1	343.5

[a] more detailed values are given in the caption of Figure 2.

In comparison with the experimental X-ray diffraction (XRD) data, Table 1 shows selected geometry parameters of the **qGe** and **qGe⁺**. Note that Siemeling *et al.*[27] also found a second, strongly distorted, thermodynamically disfavoured (ΔG = 20.5 kcal mol^{-1}) bent structure for Fc(NMes)$_2$Ge, which was, however, not considered in our study. The agreement between computed bond lengths for **qGe** and experiment (**4**) is satisfactory (**4$^+$** is not known yet). The structural changes upon going from **qGe** to **qGe$^+$** are relatively small, in accordance with Siemeling *et al.*[27] The (mostly) germanium-centered lone-pair of electrons for the NHGe **qGe** was found to be HOMO−4, *i.e.* much lower than typically found for the related NHC derivatives,[11] whereas the lowest unoccupied molecular orbital (LUMO) represents the expected p-type acceptor orbital of the germylene. Note that Figure 9a displays this Ge(4p) orbital analogous to the schematic drawing in Scheme 2.

The HOMO (not shown) is centered on the iron atom of the ferrocene backbone of **qGe**. Furthermore, spin density calculations on the optimized geometry of the cationic germylene **qGe$^+$** clearly suggests that the oxidation process seen in the cyclic voltammogramm of **4** (*cf.* Figure 3) is also located on the iron center (Figure 9b). Natural population analyses (NPA) further support these findings (**qGe**: Fe: +0.25, Ge: +1.11; **qGe$^+$**: Fe: +1.23, Ge: +0.01). These computational results nicely confirm the above mentioned view of a redox-switchable germylene metalloligand.

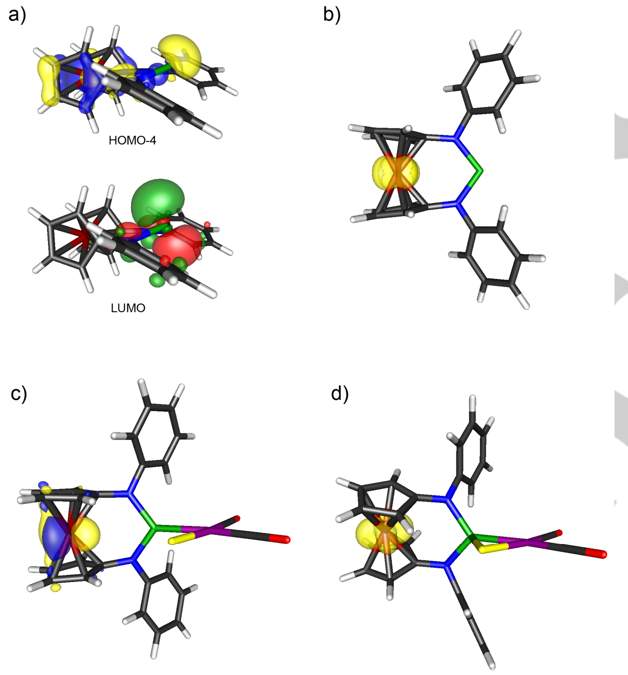

Figure 9. Selected frontier orbitals of **qGe** (a), spin density of **qGe$^+$** (b), HOMO of [Rh(κ^1*Ge*-**qGe**)(CO)$_2$Cl] (**qGeRh**, c), and spin density of [Rh(κ^1*Ge*-**qGe**)(CO)$_2$Cl]$^+$ (**qGeRh$^+$**, d) obtained at the B3LYP/def2-TZVP level (C: black; H: grey; N: blue; Cl: yellow; O: red; Fe: dark red; Ge: green). Note that for all calculated model compounds the Mes substituents have been replaced by Ph. For clarity reasons, we have only displayed positive spin density in the contour plots b) and d). Small negative spin populations reside in all cases on the C atoms of the Cp rings.

In order to compare the results obtained for **qGe** and **qGe$^+$** with the so-far unknown silicon derivatives and the previously described **FcDAC** mentioned in the introduction, we have also calculated the model compounds **qSi**/**qSi$^+$** and **qC**/**qC$^+$** (see Section S4 of the Supporting Information). As expected, the calculated energies of the σ-donor and π-acceptor orbitals centered on the ylene unit of the neutral model compounds **qC**, **qSi**, and **qGe** strongly decrease upon descending the Group 14 (*cf.* Figure 10, Table 2).

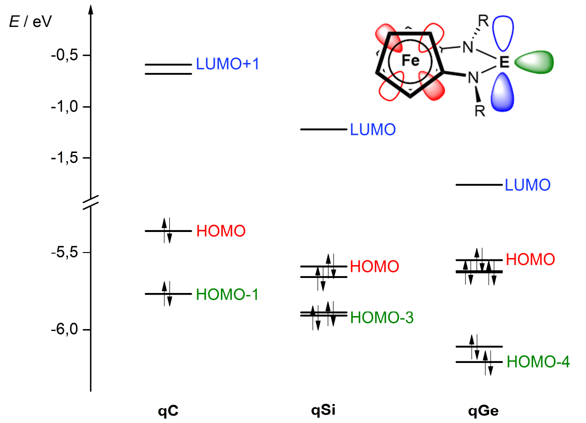

Figure 10. Compilation of the calculated orbital energies of **qC**, **qSi** and **qGe** obtained at the B3LYP/def2-TZVP level; simplified visualization of the π-acceptor orbital (blue), the iron-centered HOMO (red) and the σ-donor orbital of the ylene unit (green).

The results nicely correspond to orbital diagrams of benzo-anellated NHC, NHSi, and NHGe compounds presented by Heinicke *et al.*[44] The energy of the Fe-centered HOMO changes only slightly within this series[46] and, consistently, the spin density is located almost exclusively on the iron atom in the cationic species **qE$^+$**. Note that previous reports of Siemeling and co-workers on the carbene system showed a slightly more delocalized nature with the spin density distributed across the iron and the carbene carbon atom.[27,11c]

Table 2. Calculated orbital energies [eV] of **qC**, **qSi** and **qGe** obtained at the B3LYP/def2-TZVP level.

model comp.	π-acceptor (ylene)	HOMO (Fe)	σ-donor (ylene)
qC	-0.59[b]	-5.36	-5.77[c]
qSi	-1.22[a]	-5.59	-5.91[d]
qGe	-1.76[a]	-5.55	-6.21[e]

[a] LUMO; [b] LUMO+1; [c] HOMO-1; [d] HOMO-3; [e] HOMO-4

Table 3. Selected geometry parameters (bond lengths in pm, angles in °) of the model compounds **qERh**/**qERh$^+$** with E = C, Si, Ge.

Compound	avg. Fe-C	avg. E-N	N-E-N	E-Rh	Rh-Cl	E···Cl
qGeRh	206.7	185.5	108.1	243.7	240.8	269.0
qGeRh$^+$	211.7	188.7	104.9	241.8	244.2	253.8
qSiRh	206.6	173.1	111.9	231.9	245.5	236.9
qSiRh$^+$	212.1	175.3	107.3	229.2	249.6	228.3
qCRh	205.5	134.8	122.8	211.6	240.6	306.7
qCRh$^+$	210.8	135.2	122.3	209.4	241.8	289.2

To further explore the electronic alteration of the metalloligand upon oxidation, we investigated in a next step the (hypothetical) Rh(CO)$_2$Cl complex of **4**, namely [Rh(κ^1*Ge*-**qGe**)(CO)$_2$Cl] (**qGeRh**) and its cationic counterpart **qGeRh$^+$** (Figure 9c and d, respectively). Table 3 shows selected geometry parameters. Most notably, the structural differences between **qGeRh** and **qGeRh$^+$**

10.1002/chem.201605073

are much more pronounced as compared to the couple **qGe**/**qGe⁺**, in particular the tilting of the N-Ph entities with respect to the planes defined by the Cp ligands (see Figure 9c and d). Furthermore, the oxidized complex **qGeRh⁺** shows a relatively short contact between Ge and Cl of 253.8 pm (*cf.* 269.0 pm for **qGeRh**). This structural aspect already hints to a significant increase of the acceptor properties of the germanium(II) atom. Again, spin density calculations verified the hypothesis of an Fe-centered redox process (Figure 9d). Most importantly, the calculated CO stretching frequencies considerably change from ν_1^{calc} = 2073 cm^{-1} and ν_2^{calc} = 2008 cm^{-1} for **qGeRh** (ν_{av}^{calc} = 2041 cm^{-1}) to ν_1^{calc}= 2102 cm^{-1} and ν_2^{calc}= 2044 cm^{-1} in **qGeRh⁺** (ν_{av}^{calc} = 2073 cm^{-1}). Although these computed vibrational frequencies ν_{av}^{calc} had to be scaled in order to be compared with experimental values,[47] the ν_{av}^{calc} data appear to suffer from a systematic error because the calculated data would justify a categorization of the germylene (**4**) among good donor ligands if compared to $Rh(CO)_2Cl$ complexes of both electron-rich and electron-deficient NHC ligands.[48,19d] For the above mentioned ν_{av}^{calc} values a TEP_{qGe}^{calc} for **qGe** of 2051 cm^{-1} would result (Table 4).[49] This would be comparable to classical NHC ligands like IAd or IPr. However, the calculated orbital energies for the series **qC**, **qSi** and **qGe** clearly showed that **qGe** should be a (much) *weaker* donor as compared to **qC**, for instance, which would also be in line with the common view in the literature.[50]

In order to overcome this problem, we have again also calculated the lighter congeners, namely **qSiRh** and **qCRh**, both for comparison and, more importantly, to calibrate the results obtained for this series with the experiment, which is known for the $[Rh(CO)_2Cl]$ complex of **FcDAC** (TEP_{FcDAC}^{exp} = 2048.5 cm^{-1}).[11] A direct comparison of TEP_{FcDAC}^{exp} with the calculated TEP_{qC}^{calc} of 2040 cm^{-1} gave the correction factor F = 1.0039 (and this TEP_{qC}^{corr} = 2049 cm^{-1}).[51] The correction was applied to all model compounds to furnish TEP_{qSi}^{corr} of 2052 cm^{-1} and TEP_{qGe}^{corr} of 2059 cm^{-1}, respectively (Table 4). To put these numbers into perspective, the genuine carbene ligand **FcDAC** shows donor properties comparable to classical NHC ligands like IAd (Figure 11). The so-far unknown silicon derivative **qSi** is still a good donor, in the range of electron-rich phosphine ligands such as $PCyc_3$ or the carbene IPr (Figure 11). As expected, the germanium compound **qGe** is a weaker ligand and falls in the typical region found for phosphine ligands such as P*i*Pr_3 or $PCyc_3$ (Figure 11).

Table 4. Calculated TEP_{qE}^{corr} and TEP_{qE+}^{corr} values [cm^{-1}] using a correction factor of F = 1.0039 in order to calibrate the calculated results with the experiment.

model comp.	TEP_{qE}^{corr}	TEP_{qE+}^{corr}	$\Delta TEP_{qE/qE+}^{corr}$
qC/qC⁺	2049[a]	2069	20
qSi/qSi⁺	2052	2077	25
qGe/qGe⁺	2059	2084	25

[*a*] calibrated to the experiment, TEP_{FcDAC}^{exp} = 2048.5 cm^{-1}.

Last but not least, we were very much interested in estimating the difference in the TEP values upon switching the redox-state of the metalloligands. Table 4 summarizes the TEP_{qE+}^{corr} of the oxidized ylenes **qC⁺**, **qSi⁺** and **qGe⁺** in the complexes **qCRh⁺**, **qSiRh⁺** and **qGeRh⁺**, respectively. Most notably, upon *in silico* one-electron oxidation to **qERh⁺**, the TEP_{qE+}^{corr} values for all model compounds are significantly increased by 20-25 cm^{-1} to 2069 cm^{-1} for **qC⁺**, 2077 cm^{-1} for **qSi⁺**, and 2084 cm^{-1} for **qGe⁺**, respectively. As experimental ΔTEP^{exp} values of only up to *ca.* 11 cm^{-1} have been reported, it appears that these calculated data for the gas-phase species overestimate the effect of changing the redox-state of the ligand. However, the former are solution processes, which are much more complicated considering, for instance, the influence of the solvent, the counter anions, etc. Nevertheless, the qualitative trend to decreasing the donor and/or increasing the acceptor properties of metalloligands upon oxidation is clear. For our compound of interest, *i.e.* the redox-switchable germylene, the calculated ligation properties for **qGe⁺** (TEP_{qE+}^{corr} = 2084 cm^{-1}) is in the range of phosphite ligands and very electron-deficient phosphines such as $P(C_6F_5)_3$ (TEP^{exp} = 2090.9 cm^{-1}). Note that Kühl *et al.*[50] has nicely shown by comprehensive calculations of NHGe derivatives that such TEP values can only be achieved by introducing strong acceptor substituents like cyano or nitro groups In our case, however, such values are accessible by simply removing one electron from the redox-switchable germylene.

Considering the above mentioned overestimation for the gas-phase calculation by the factor of *ca.* 2, we expect the experimentally determined, solution-based TEP value for the cationic germylene to be in the region of electron-deficient phosphines and phosphites, *i.e.* around 2072 cm^{-1}. This has, however, to be confirmed by experiment, which is in the current focus of our interest.

We also note in passing that the increase of the TEP values upon oxidation is slightly more pronounced for the heavier ylenes as compared to the carbene ligand. Although it is too early for a final statement, this might be due to a better orbital overlap in these polynuclear scaffolds induced by the larger valence orbitals of the donor atom, in this case the 3p and 4p acceptor orbitals of silicon and germanium, respectively. Nevertheless, the change in the ligand donating abilities upon oxidation can, as previously noted,[20] mainly be attributed to Coulombic effects while an orbital-based interaction appears to have only a minor influence.

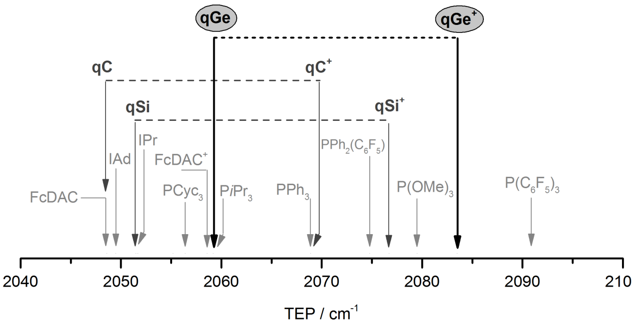

Figure 11. Tolman electronic parameter (TEP) of **qE** and **qE⁺** (*calculated*, E = C, Si, Ge) and selected NHC and phosphine ligands (*experimental* values taken from the literature).

Conclusions

In this work we have described the synthesis and characterization of a redox-switchable germylene based on a 1,1'-ferrocenediyl backbone, $[Fc(NMes)_2Ge]$ (**4**), which is readily available from $Fc(NHMes)_2$ (**2**) and $Ge\{N(SiMe_3)_2\}_2$, or from the dilithiated compound $Fc(NLiMes)_2 \cdot 3\ Et_2O$ (**3**) and $GeCl_2$ in 61 and 33 % isolated yield, respectively. The calculated buried volume (%V_{bur}) of **4** amounts to 39.2 and reasonably compares with those reported for the Fc-based NHC derivatives. Cyclic voltammetry studies are provided for **4** confirming the above mentioned view of a redox-switchable germylene metalloligand. Several attempts to isolate the 1:1 Rh(I) and Ir(I) complexes of **4**, [Rh(κ^1*Ge*-**4**)(cod)Cl] (**5**), [Ir(κ^1*Ge*-**4**)(cod)Cl] (**6**), and [Ir(κ^1*Ge*-**4**)(CO)$_2$Cl] (**7**), failed so far. However, as evidenced with the aid of various NMR spectroscopic techniques, all complexes are cleanly formed in solution. On the other hand, the 1:2 metal-ligand complexes [Mo(κ^1*Ge*-**4**)$_2$(CO)$_4$] (**8**) and [W(κ^1*Ge*-**4**)$_2$(CO)$_4$] (**9**) are stable and were isolated in 49 % and 14 % yield, respectively. The structural parameters of **8** were determined by X-ray diffraction showing a *trans* arrangement of both germylene ligands. The local D_{4h} symmetry around the metal atom in **8** and **9** were also confirmed by IR and Raman investigations. Density functional theory (DFT) calculations have been provided on a series of model compounds in order to elucidate a conceivable interplay between the metal atoms in bimetallic complexes of the type [Rh(κ^1*E*-**qE**)(CO)$_2$Cl]$^{0/+}$ (E = C, Si, Ge). The bonding characteristics of the coordinated Fc-based metalloligands (**qE**/**qE$^+$**) are strongly affected upon *in silico* oxidation of the calculated complexes. The calculated Tolman electronic parameter (TEP) significantly increase by 20-25 cm^{-1} upon oxidation. Although this dependence suggests an interaction between both metals due to their close spatial proximity, only small differences in the ΔTEP values have been observed by substituting the carbene (E = C; ΔTEP = 20 cm^{-1}) for the silylene or the germylene (E = Si, Ge; ΔTEP = 25 cm^{-1}). The change in the ligand donating abilities upon oxidation can thus mainly be attributed to Coulombic effects, while an orbital-based interaction appears to have only a minor influence.

Experimental Section

General methods and instrumentation. The reactions were performed under an inert atmosphere of argon using Schlenk techniques, unless stated otherwise. Air sensitive compounds were stored and weighed in a glovebox. All solvents (THF, toluene, benzene) were freshly distilled under argon from sodium/benzophenone (THF, benzene, toluene) prior to use. Diethyl ether was distilled from sodium/potassium alloy/benzophenone immediately prior use. [D$_8$]THF and C_6D_6 were vacuum transferred from potassium/benzophenone into thoroughly dried glassware equipped with Young teflon valves. Elemental analyses were carried out in the institutional technical laboratories of the Karlsruhe Institute of Technology (KIT). Due to the air- and moisture-sensitive nature of **3**, no satisfactory elemental analyses could be obtained. For the complexes **8** and **9**, the obtained results are outside the range viewed as establishing analytical purity. This is due to the varying solvent content of crystalline samples dried *in vacuo*. IR spectra were recorded on a Bruker Alpha spectrometer in the range from 4000 cm^{-1} to 400 cm^{-1} using a KBr beamsplitter. Samples were measured by using the ATR technique (attenuated total reflection) on bulk material, and the data are quoted in wavenumbers (cm^{-1}). The intensity of the absorption band is indicated as vw (very weak), w (weak), m (medium), s (strong), vs (very strong), and br (broad). FT-Raman spectra were taken using a Bruker MultiRam spectrometer; the excitation wavelength of the Nd-YAG laser was 1064 nm. Cyclic voltammetry measurements were performed with a suitable potentiostat and an electrochemical cell within a glovebox. We used a freshly polished Pt disk working electrode, a Pt wire as counter electrode, and a Ag wire as (pseudo) reference electrode {[*n*Bu$_4$N][PF$_6$] (0.05 M) or [*n*Bu$_4$N][Al{OC(CF$_3$)$_3$}$_4$] (0.05 M) as electrolyte}. Potentials were calibrated against the Fc/Fc$^+$ couple (internal standard). UV-VIS spectra were recorded in dry THF on a Varian Cary 100 Scan spectrometer in the range from 800 nm to 260 nm using a quarz cuvette (d = 1 cm). Solution NMR spectra were recorded with NMR instruments operating at ^{1}H Larmor frequencies of 300 and 400 MHz. The spectral reference used was TMS for ^{1}H and ^{13}C. Coupling constants *J* are given in Hertz as positive values regardless of their real individual signs. The multiplicity of the signals is indicated as s, d, q, or m for singlets, doublets, quartets, or multiplets, respectively. The abbreviation br. is given for broadened signals. Assignments were confirmed if necessary with the use of two-dimensional correlation experiments. Pulsed field-gradient spin-echo (PGSE) measurements were conducted as previously described.[52] All diffusion and molecular size estimations were performed using the DiffAtOnce software package.[52c]

Computational details. The calculations were performed with the TURBOMOLE program package[53] in the framework of density functional theory (DFT). The functional B3LYP[54] was used in conjunction with the def2-TZVP basis sets.[55] Vibrational frequencies were computed by using Turbomole's module Aoforce.

Starting materials. Fc(NH$_2$)$_2$ (**1**) was prepared according to literature procedures.[30] The different transition metal compounds employed were used as obtained from commercial sources without further purification.

2:[31] A mixture of Pd$_2$dba$_3$ (672 mg, 0.73 mmol) and dppf (630 mg, 1.14 mmol) in toluene (70 ml) was placed in a 500 ml round bottom flask. NaO*t*Bu (2.35 g, 24.50 mmol), 2-Bromomesitylene (5.87 g, 4.50 ml, 29.50 mmol) and 1,1'-*N*-ferrocenyldiamine (2.10 g, 9.72 mmol) were added subsequently to the dark orange solution. The resulting suspension was diluted with THF (140 ml) and heated to 95 °C for 64 h. The following work-up procedure was performed under air. After cooling to room temperature, the dark red suspension was poured into water (140 ml) and extracted 5 times with 200 ml of diethyl ether. The combined ethereal layers were dried over magnesium sulfate. All volatile components were removed *in vacuo*. The red oily residue was taken up in diethyl ether and filtered through a pad of Florisil®. After reducing the filtrate to dryness, the residue dissolved in dry toluene (15 ml). **2** was collected as a brownish, micro crystalline solid (2.23 g, 4.93 mmol, 51 %) at -40 °C. Suitable crystals for X-ray diffraction can be obtained by recrystallization from diethyl ether. ^{1}H NMR (300.1 MHz, C_6D_6, 25°C): δ = 2.12 (s, 12 H, Mes-oC***H***$_3$), 2.17 (s, 6 H, Mes-pC***H***$_3$), 3.78 (m, 4 H, Cp-C***H***(2,5)), 3.81 (m, Cp-CH(3,4)), 4.05 (s, 2 H, N***H***, $W_{1/2}$ = 3.5 Hz), 6.78 (s, Mes-C***H***). ^{13}C NMR (75.5 MHz, C_6D_6, 25°C): δ = 18.7 (s, Mes-o***C***H$_3$), 20.8 (s, Mes-p***C***H$_3$), 60.3 (s, Cp-***C***H(3,4)), 64.6 (s, Cp-***C***H(2,5)), 108.2 (s, Cp-***C***(1)), 129.9 (s, Mes-***C***-oCH$_3$), 131.0 (s, Mes-***C***H), 132.4 (s, Mes-***C***-pCH$_3$), 139.8 (s, N-***C***-Mes). FT-IR (ATR): v = 410 s, 429 s, 449 vs, 458 s, 484 s, 501 m, 510 m, 526 w, 558 m, 578 w, 602 w, 614 w, 646 w, 664 w, 693 m, 729 w, 763 w, 800 s, 838 m, 858 s, 882 w, 937 m, 958 w, 1009 s, 1029 w, 1037 m, 1051 w, 1063 vw, 1098 vw, 1122 w, 1155 w, 1221 m, 1261 s, 1276 w, 1305 m, 1347 w, 1377 m, 1435 m, 1471 s, 1500 vs, 1586 vw, 1736 vw, 1776 vw, 2732 br, vw, 2853 w, 2910 w, 2941 w, 2962 vw, 3024 vw, 3083 vw, 3096 vw, 3404 m cm^{-1}.

3: A solution of **2** (2.00 g, 4.42 mmol) in diethyl ether (80 ml) was treated carefully with BuLi in hexane (2.50 M, 3.90 mL, 9.73 mmol) at -78 °C. The resulting suspension was raised to ambient temperature and stirred for 18 h. The yellowish orange precipitate was filtered, washed twice with diethyl ether (10 ml) and dried *in vacuo*. The content of ether was determined (3 diethyl ether molecules per ferrocenyl moiety) by ^{1}H NMR measurements in C_6D_6 (yield: 1.256 g, 1.82 mmol, 41 %). M. p. (sealed tube under Ar): >189°C (dec.). ^{1}H NMR (300.1 MHz, C_6D_6, 25°C): δ = 1.11 (t, 18 H, (C***H***$_3$CH$_2$)$_2$O), 2.09 (s, 6 H, Mes-oC***H***$_3$), 2.12 (s, 6 H, Mes-oC***H***$_3$), 2.46 (s, 6 H, Mes-pC***H***$_3$), 2.96 (m, 2 H, Cp-C***H***), 3.26 (q, 12 H, (CH$_3$C***H***$_2$)$_2$O), 3.38 (m, 2 H, Cp-C***H***), 3.54 (m, 2 H, Cp-C***H***) 3.73 (m, 2H, Cp-C***H***), 6.91 (s, 2 H, Mes-C***H***), 7.23 (s, Mes-C***H***). ^{7}Li NMR (116.6 MHz, C_6D_6, 25°C): δ = 2.6 (s, broad, **Li**), 0.9 (s, broad, **Li**). ^{13}C NMR (75.5 MHz, C_6D_6, 25°C): δ [ppm] = 15.1 ((***C***H$_3$CH$_2$)$_2$O), 19.0 (2 signals, Mes-o***C***H$_3$), 20.6 (Mes-p***C***H$_3$), 55.0 (Cp-***C***H), 58.8 (Cp-***C***H), 62.3 (Cp-***C***H), 64.1 (Cp-***C***H), 65.5 ((CH$_3$***C***H$_2$)$_2$O), not detected (Cp-***C***(1), 130.2 (Mes-***C***H), 131.6 (Mes-***C***H), 130.8 (s, Mes-***C***-oCH$_3$), 133.9 (s, Mes-***C***-oCH$_3$), 133.6 (Mes-***C***-pCH$_3$), 149.8 (N-***C***-Mes). FT-IR (ATR): v = 443 s, 460 s, 449 vs, 489 m, 507 m, 534 s, 561 s, 580 m, 607 w, 632 m, 643 m, 686 w, 710 w, 735 w, 761 w, 772 m, 782 m, 791 m, 806 s, 824 w, 853 s, 880 w, 916 w, 936 m, 957 w, 977 vw, 1002 w, 1021 m, 1046 m, 1069 br, m, 1100 w, 1150 m, 1200 m, 1219 m, 1243 s, 1264 s, 1298 m, 1323 w, 1356 w, 1375 m, 1387 m, 1422 m, 1454 vs, 1518 br, vw, 1607 br, vw, 1726 vw, 2727 br, vw, 2857 vw, 2873 vw, 2910 vw, 2923 w, 2968 w, 3020 vw, 3073 vw, 3082 vw, 3094 vw, 3130 vw cm^{-1}. Elemental analysis: varying values.

4: *Route 1*: During a time period of 15 min, a solution of $GeCl_2$ (424 mg, 1.83 mmol) in toluene (40 ml) was added dropwise to a suspension of **3** (1.256 g, 1.83 mmol) in toluene (60 ml) at -78 °C. The mixture was brought to ambient temperature and stirred for 18 h. The red brownish suspension was filtered. All volatile components of the filtrate were removed *in vacuo* and diethyl ether (30 ml) was added. A further filtration provided the separation of a greyish green precipitate from the red filtrate. The volume of the filtrate was reduced and compound **4** was obtained as a red, crystalline solid at -40 °C (255 mg, 0.49 mmol, 27 %). A second crop of **4** was obtained by further concentration of the mother liquor (65 mg, 0.12 mmol, 7 %). Total yield: 320 mg, 0.61 mmol, 33 %.

Route 2: A mixture of $Ge\{N(SiMe_3)_2\}_2$ (197 mg, 0.50 mmol) and **2** (226 mg, 0.50 mmol) in toluene (10 ml) was stirred 14 days at 60 °C. All volatile components were removed *in vacuo* and was crystallized from diethyl ether at -40 °C (5 ml). **4** was obtained as orange prisms (160 mg, 0.31 mmol, 61 %). M. p. (sealed tube under Ar): 235-237°C. ^1H NMR (300.1 MHz, C_6D_6, 25°C): *δ* = 2.13 (s, 6 H, Mes-pC***H***$_3$), 2.49 (s, 12 H, Mes-oC***H***$_3$), 3.89 and 4.33 (AA'BB' spin system, ^3J[1,1] = 1.04 Hz, ^3J[1,2] = 2.67 Hz, ^3J[2,1] = 1.17 Hz, ^3J[2,2] = 5.14 Hz, 2 × 4 H, Cp-C***H***(3,4) and Cp-C***H***(2,5), see the Supporting Information), 6.81 (s, 4 H, Mes-C***H***). ^1H NMR (300.1 MHz, [D$_8$]THF, 25°C): *δ* = 2.20 (s, 6 H, Mes-pC***H***$_3$), 2.47 (s, 12 H, Mes-oC***H***$_3$), 3.93 and 4.35 (AA'BB' spin system, ^3J[1,1] = 1.04 Hz, ^3J[1,2] = 2.67 Hz, ^3J[2,1] = 1.17 Hz, ^3J[2,2] = 5.14 Hz, 2 × 4 H, Cp-C***H***(3,4) and Cp-C***H***(2,5), see the Supporting Information), 6.87 (m, 4 H, Mes-C***H***). ^{13}C NMR (75.5 MHz, C_6D_6, 25°C): *δ* = 20.5 (s, Mes-o***C***H$_3$), 21.3 (s, Mes-p***C***H$_3$), 67.4 (s, Cp-***C***H(3,4)), 68.4 (s, Cp-***C***H(2,5)), 109.6 (s, Cp-***C***(1)), 130.3 (s, Mes-***C***-oCH$_3$), 135.5 (s, Mes-***C***H), 137.3 (s, Mes-***C***-pCH$_3$), 143.7 (s, N-***C***-Mes). ^{13}C NMR (75.5 MHz, [D$_8$]THF, 25°C): *δ* = 20.3 (s, Mes-o***C***H$_3$), 20.9 (s, Mes-p***C***H$_3$), 67.2 (s, Cp-***C***H(3,4)), 68.4 (s, Cp-***C***H(2,5)), 109.9 (s, Cp-***C***(1)), 130.1 (s, Mes-***C***-oCH$_3$), 135.7 (s, Mes-***C***H), 137.5 (s, Mes-***C***-pCH$_3$), 144.0 (s, N-***C***-Mes). FT-IR (ATR): ν = 416 m, 458 m, 490 s, 508 m, 522 s, 534 m, 560 s, 579 w, 594 w, 637 m, 644 m, 716 w, 764 w, 799 s, 837 m, 848 m, 861 w, 881 s, 946 s, 1011 m, 1020 m, 1037 w, 1071 vw, 1123 w, 1144 s, 1194 s, 1223 w, 1257 m, 1303 w, 1331 w, 1372 m, 1445 s, 1474 m, 1504 w, 1595 vw, 1607 vw, 1629 vw, 1667 vw, 1729 vw, 1769 vw, 2727 vw, 2851 w, 2912 w, 2941 w, 2974 w, 3081 vw, 3098 vw, 3404 w cm^{-1}. UV-VIS (THF): λ_{max} (ε): 456 nm (ε = 962 dm^{3}mol^{-1}cm^{-1}), 294 nm (ε = 16360 dm^{3}mol^{-1}cm^{-1}). Elemental analysis: $C_{28}H_{30}FeGeN_2$ (523.03); C 64.54 (calcd. 64.30); H 5.76 (5.78); N 5.35 (5.36) %.

5: In a typical experiment, a mixture of **4** (15.7 mg, 0.03 mmol) and [Rh(COD)Cl]$_2$ (7,4 mg, 0,015 mmol) were dissolved in C_6D_6 ([D$_8$]THF) (0.7 ml) in a *J. Young* NMR tube. The selectively formed compound **5** could not be isolated since decomposition takes place in the process of *in vacuo* solvent removal. ^1H NMR (400.1 MHz, C_6D_6, 25°C): *δ* = 1.29 (m, 2 H, COD-C***H***$_2$), 1.41 (m, 2 H, COD-C***H***$_2$), 1.56 (m, 2 H, COD-C***H***$_2$), 1.61 (m, 2 H, COD-C***H***$_2$), 2.15 (s, 6 H, Mes-pC***H***$_3$), 2.65 (s, 12 H, Mes-oC***H***$_3$), 3.79 (m, 2 H, COD-C***H***), 3.86 and 4.39 (AA'BB' spin system, 2 × 4 H, Cp-C***H***(3,4) and Cp-C***H***(2,5)), 5.05 (m, 2 H, COD-C***H***), 6.84 (s, 4 H, Mes-C***H***). ^1H NMR (400.1 MHz, [D$_8$]THF, 25 °C): δ = 1.49-1.87 (m, 8 H, COD-C***H***$_2$), 2.25 (s, 6 H, Mes-pC***H***$_3$), 2.50 (s, 12 H, Mes-oC***H***$_3$), 3.65 (m, 2 H, COD-C***H***), 4.00 (m, 4 H, Cp-C***H***(3,4)), 4.43 (m, 4H, Cp-C***H***(2,5)), 4.71 (m, 2 H, COD-C***H***). ^{13}C NMR (100.6 MHz, C_6D_6, 25°C): *δ* = 20.5 (s, broad, Mes-o***C***H$_3$), 20.9 (s, Mes-p***C***H$_3$), 28.3 (s, COD-***C***H$_2$), 33.3 (s, COD-***C***H$_2$), 67.6 (d, $^1J_{C,Rh}$ = 13.1 Hz, broad, COD-***C***H), 67.7 (s, broad, Cp-***C***H(3,4)), 68.6 (s, broad, Cp-***C***H(2,5)), 99.5 (d, $^1J_{C,Rh}$ = 8.7 Hz, broad, COD-***C***H), 105.1 (s, broad, Cp-***C***(1)), 130.0 (s, Mes-***C***-oCH$_3$), 136.0 (s, Mes-***C***H), 137.8 (s, Mes-***C***-pCH$_3$), 142.2 (s, N-***C***-Mes).

6: In a typical run, a mixture of **4** (15.7 mg, 0.03 mmol) and [Ir(COD)Cl]$_2$ (10.1 mg, 0,015 mmol) were solved in C_6D_6 ([D$_8$]THF) (0.7 ml) in a *J. Young* NMR tube. The selectively formed compound 5 could not be isolated since decomposition takes place in the process of *in vacuo* solvent removal. ^1H NMR (400.1 MHz, C_6D_6, 25°C): δ = 1.00 (m, 2 H, COD-C***H***$_2$), 1.21 (m, 2 H, COD-C***H***$_2$), 1.39 (m, 2 H, COD-C***H***$_2$), 1.59 (m, 2 H, COD-C***H***$_2$), 2.12 (s, 6 H, Mes-pC***H***$_3$), 2.63 (s, 12 H, Mes-oC***H***$_3$), 3.61 (m, 2 H, COD-C***H***), 3.84 (m, 4 H, Cp-C***H***(3,4)), 4.33 (m, 4H, Cp-C***H***(2,5)), 4.72 (m, 2 H, COD-C***H***), 6.81 (s, 4 H, Mes-C***H***). ^1H NMR (400.1 MHz, [D$_8$]THF, 25°C): δ = 1.19 (m, 2 H, COD-C***H***$_2$), 1.30 (m, 2 H, COD-C***H***$_2$), 1.52 (m, 4 H, COD-C***H***$_2$), 2.24 (s, 6 H, Mes-pC***H***$_3$), 2.52 (s, 12 H, Mes-oC***H***$_3$), 3.45 (m, 2 H, COD-C***H***), 4.04 (m, 4 H, Cp-C***H***(3,4)), 4.31 (m, 2 H, COD-C***H***), 4.47 (m, 4H, Cp-C***H***(2,5)), 6.90 (s, 4 H, Mes-C***H***). ^{13}C NMR (75.5 MHz, C_6D_6, 25°C): δ = 20.3 (s, Mes-o***C***H$_3$), 20.9 (s, Mes-p***C***H$_3$), 29.0 (s, COD-***C***H$_2$), 34.4 (s, COD-***C***H$_2$), 50.8 (s, COD-***C***H), 67.9 (s, Cp-***C***H(3,4)), 68.6 (s, Cp-***C***H(2,5)), 87.8 (s, COD-***C***H), 104.9 (s, Cp-***C***(1)), 130.1 (s, Mes-***C***-oCH$_3$), 136.2 (s, Mes-***C***H), 137.3 (s, Mes-***C***-pCH$_3$), 141.9 (s, N-***C***-Mes). ^{13}C NMR (75.5 MHz, [D$_8$]THF, 25°C): *δ* = 20.4 (s, Mes-o***C***H$_3$), 21.0 (s, Mes-p***C***H$_3$), 29.6 (s, COD-***C***H$_2$), 34.9 (s, COD-***C***H$_2$), 51.5 (s, COD-***C***H), 68.2 (s, Cp-***C***H(3,4)), 69.1 (s, Cp-***C***H(2,5)), 87.3 (s, COD-***C***H), 105.6 (s, Cp-***C***(1)), 130.2 (s, Mes-***C***-oCH$_3$), 136.7 (s, Mes-***C***H), 137.9 (s, Mes-***C***-pCH$_3$), 142.4 (s, N-***C***-Mes).

7: In a *J. Young* NMR tube, a mixture of **4** (24.0 mg, 0.05 mmol) and [Ir(COD)Cl]$_2$ (12.4 mg, 0.018 mmol) were dissolved in [D$_8$]THF (0.7 ml). The solution was degassed by three cycles of a freeze-pump-thaw procedure using liquid nitrogen. The frozen mixture was treated with ~ 1.5 bar of carbon monoxide. After allowing to warm to ambient temperature, a color change from red to reddish orange took place. The selectively formed compound **7** could not be isolated since decomposition takes place in the process of *in vacuo* solvent removal. ^1H NMR (400.1 MHz, [D$_8$]THF, 25°C): *δ* = 2.18 (s, 6 H, Mes-pC***H***$_3$), 2.33 (m, broad, 8 H, free COD-C***H***$_2$), 2.56 (s, 6 H, Mes-oC***H***$_3$), 2.64 (s, 6 H, Mes-oC***H***$_3$), 3.88 (m, 2 H, Cp-C***H***), 4.10 (m, 2 H, Cp-C***H***), 4.38 (m, 2 H, Cp-C***H***), 4.77 (m, 4H, Cp-C***H***), 5.50 (m, 4 H, free COD-C***H***), 6.75 (s, 4 H, Mes-C***H***), 6.85 (s, 4 H, Mes-C***H***). ^{13}C NMR (100.6 MHz, [D$_8$]THF, 25°C): *δ* = 20.9 (s, Mes-o***C***H$_3$), 21.2 (s, Mes-o***C***H$_3$), 21.5 (s, Mes-p***C***H$_3$), 28.9 (s, free COD-***C***H$_2$), 66.8 (s, Cp-***C***H(3,4)), 68.2 (s, Cp-***C***H(2,5)), 68.4 (s, Cp-***C***H(2,5)), 71.3 (s, free COD-***C***H), 103.8 (s, Cp-***C***(1)), 130.0 (s, Mes-***C***-oCH$_3$), 130,.8 (s, Mes-***C***-oCH$_3$), 136.7 (s, Mes-***C***H), 138.6 (s, Mes-***C***H), 141.6 (s, Mes-***C***-pCH$_3$), 144.4 (s, N-***C***-Mes) 166.0 (s, ***C***O), 185.2 (s, ***C***O).

8: **4** (100 mg, 0.19 mmol) and $Mo(CO)_6$ (26 mg, 0.10 mmol) were dissolved in THF (10 ml). The mixture was irradiated for 2 h with a mercury vapor lamp while being stirred. Orange, rod shaped crystals of **8** were isolated by layering the solution with hexane (20 ml) (59 mg, 0.047 mmol, 49 %). M. p. (sealed tube under Ar): 233 – 235°C (dec.). ^1H NMR (400.1 MHz, C_6D_6, 25°C): *δ* = 2.15 (s, 12 H, Mes-pC***H***$_3$), 2.47 (s, 24 H, Mes-oC***H***$_3$), 3.77 and 4.18 (AA'BB' spin system, 2 × 4 H, Cp-C***H***(3,4) and Cp-C***H***(2,5)), 6.81 (s, 8 H, Mes-C***H***). **^{13}C NMR** (100.6 MHz, C_6D_6, 25°C): *δ* = 20.1 (s, Mes-o***C***H$_3$), 21.0 (s, Mes-p***C***H$_3$), 67.6 (s, broad, Cp-***C***H(3,4), Cp-***C***H(2,5)), 106.1 (s, Cp-***C***(1)), 130.5 (s, Mes-***C***-oCH$_3$), 135.9 (s, Mes-***C***H), 137.0 (s, Mes-*C*-pCH$_3$), 143.1 (s, N-*C*-Mes), 207.7 (s, Mo-*C*O). **FT-IR** (**ATR**): ν = 403 s, 440 m, 452 m, 491 s, 506 s, 522 s, 541 s, 560 vs, 580 m, 606 vs, 647 s, 716 m, 786 s, 804 s, 818 m, 850 m, 887 s, 914 m, 944 s, 1024 m, 1036 m, 1068 m, 1145 s, 1198 s, 1209 m, 1249 s, 1303 w, 1335 w, 1372 s, 1392 w, 1443 br, s, 1475 m, 1536 w, 1608 w, 1731 w, 1760 w, 1772 w, 1916 vs, 2035 vw, 2075 vw, 2115 vw, 2148 vw, 2727 w, 2854 w, 2917 m, 2948 w, 2999 w, 3086 w, 3101 w cm^{-1}. **Raman**: ν = 132, 236, 297, 379, 407, 422, 542, 579, 651, 890, 1058, 1152, 1215, 1252, 1303, 1375, 1447, 1609, 1971, 2038, 2918, 3088, 3107 cm^{-1}. Elemental analysis: $C_{60}H_{60}Fe_2Ge_2MoN_4O_4$ (1326.18); C 58.27 (calcd. 57.47); H 5.50 (4.82); N 3.84 (4.47) %.

9: **4** (100 mg, 0.19 mmol) and $W(CO)_6$ (34 mg, 0.10 mmol) were dissolved in THF (10 ml). The mixture was irradiated for 2 h with a mercury vapor lamp while being stirred. Orange, rod shaped crystals of **8** were isolated by layering the solution with pentane (20 ml) (18.5 mg, 0.014 mmol, 14 %). M. p. (sealed tube under Ar): 235-238°C (dec.). **^{1}H NMR** (400.1 MHz, C_6D_6, 25°C): *δ* = 2.14 (s, 12 H, Mes-pC***H***$_3$), 2.47 (s, 24 H, Mes-oC***H***$_3$), 3.77 and 4.18 (AA'BB' spin system, 2 × 4 H, Cp-C***H***(3,4) and Cp-C***H***(2,5)), 6.82 (s, 8 H, Mes-C***H***). ^{13}C NMR (100.6 MHz, C_6D_6, 25°C): *δ* = 20.2 (s, Mes-o***C***H$_3$), 21.1 (s, Mes-p***C***H$_3$), 67.7 (s, broad, Cp-***C***H(3,4), Cp-***C***H(2,5)), 105.8 (s, Cp-***C***(1)), 130.5 (s, Mes-***C***-oCH$_3$), 135.9 (s, Mes-***C***H), 137.0 (s, Mes-***C***-pCH$_3$), 143.0 (s, N-***C***-Mes), 197.7 (s, W-***C***O). **FT-IR** (**ATR**): ν = 398 s, 441 m, 454 m, 491 s, 506 m, 521 s, 541 s, 559 vs, 580 m, 600 s, 647 s, 716 m, 786 s, 803 s, 828 m, 847 m, 888 s, 944 s, 1024 s, 1037 m, 1066 m, 1145 s, 1197 s, 1209 m, 1249 br, s, 1303 w, 1335 vw, 1372 s, 1393 w, 1444 br, s, 1474 m, 1537 w, 1608 w, 1905 br, vs, 1957 w, 2024 vw, 2072 vw, 2727 vw, 2853 w, 2915 m, 2947 m, 3086 w cm^{-1}. Elemental analysis: $C_{60}H_{60}Fe_2Ge_2WN_4O_4$ (1341.95 g/mol); C 54.12 (calcd. 53.70); H 5.162 (4.51); N 3.58 (4.18) %.

Crystal structure determinations of 2, 4 and 8. Crystal data collection and processing parameters are given below. In order to avoid degradation, single crystals were mounted in perfluoropolyalkyletheroil on top of the

edge of an open Mark tube and then brought into the cold nitrogen stream of a low-temperature device (Oxford Cryosystems Cryostream unit) so that the oil solidified. Diffraction data were measured using a Stoe IPDS II diffractometer and graphite-monochromated $Mo_{K\alpha}$ (0.71073 Å) radiation. The structures were solved by dual-space direct methods with SHELXT,[56] followed by full-matrix least-squares refinement using SHELXL-2014/7.[57] All non-hydrogen atoms were refined anisotropically, with organic hydrogen atoms placed in calculated positions using a riding model. Crystals of **8** were generally of rather poor quality, reflected in the rather high R(int). The lattice solvent (7 MeCN per complex molecule) occupies cavities centred on special positions, and is badly disordered. Its contribution to the observed structure factors was calculated using SQUEEZE.[58] Structure factors therefore included contributions from the .fab file, and the quoted molecular formula includes these MeCN molecules. The structure was refined taking inversion twinning into account.
Crystallographic data (excluding structure factors) for the structures in this paper have been deposited with the Cambridge Crystallographic Data Centre as supplementary publication nos. CCDC 1497719-1497721. Copies of the data can be obtained from https://summary.ccdc.cam.ac.uk/structure-summary-form.

2: $C_{28}H_{32}FeN_2$, 452.40 g mol^{-1}, monoclinic, $P2_1/c$, a = 1453.10(11), b = 803.35(4), c = 1025.73(7) pm, β = 105.266(6)°, V = 1155.13(13) 10^6 pm^3, T = 200(2) K, Z = 2, μ(Mo-$K\alpha$) = 0.670 mm^{-1}, $D_{calcd.}$ = 1.301 g cm^{-3}; crystal dimensions 0.50×0.15×0.10 mm^3, 12455 reflections, 2753 unique data, R_{int} = 0.0457; 160 parameters, wR_2 (all data) = 0.0828, S = 1.070 (all data), R_1= 0.0303 (2307 data with $I > 2\sigma(I)$), max/min residual electron density: +0.29/–0.23 e 10^{-6} pm^{-3}.

4: $C_{28}H_{30}FeGeN_2$, monoclinic, $P2_1/c$, a = 1551.22(11), b = 1904.20(11), c = 834.31(6) pm, β = 91.128(6)°, V = 2463.9(3) 10^6 pm^3, T = 200(2) K, Z = 4, μ(Mo-$K\alpha$) = 1.826 mm^{-1}, $D_{calcd.}$ = 1.41 g cm^{-3}; crystal dimensions 0.41×0.38×0.35 mm^3, 41884 reflections, 5859 unique data, R_{int} = 0.0508; 319 parameters, wR_2 (all data) = 0.0877, S = 1.028 (all data), R_1= 0.0298 (4930 data with $I > 2\sigma(I)$), max/min residual electron density: +0.68/-0.81 e 10^{-6} pm^{-3}.

8: $C_{74}H_{81}Fe_2Ge_2MoN_{11}O_4$, 1541.31 g mol^{-1}, tetragonal, $P4_22_12$, a = 1696.1(2), , c = 1156.8(2) pm, V = 3327.8(12) 10^6 pm^3, T = 200(2) K, Z = 2, μ(Mo-$K\alpha$) = 1.562 mm^{-1}, $D_{calcd.}$ = 1.538 g cm^{-3}; crystal dimensions 0.30×0.10×0.09 mm^3, 28263 reflections, 3288 unique data, R_{int} = 0.2328; 171 parameters, wR_2 = 0.1969, S = 1.021, Flack χ = 0.44(7) (all data), R_1= 0.0739 (1919 data with $I > 2\sigma(I)$), max/min residual electron density: +0.56/–1.06 e 10^{-6} pm^{-3}.

Acknowledgements

We thank Prof. Ulrich Siemeling for his very collegial handling of the overlapping interests in this research area and Prof. Rainer Winter for very helpful comments and hints regarding the redox behaviour of the title compound. Financial support by the DFG Collaborative Research Centre CRC/Transregio 88, "Cooperative effects in homo- and heterometallic complexes (3MET)" is gratefully acknowledged (Project B4).

Keywords: Germylene • Ferrocene • Metalloligands • Redox-active Ligands

References

[1] a) A. M. Allgeier,C. A. Mirkin, *Angew. Chem. Int. Ed.* **1998**, *37*, 894; b) W. Kaim, *Inorg. Chem.* **2011**, *50*, 9752; c) P. J. Chirik, *Inorg. Chem.* **2011**, *50*, 9737; d) K. Hindson, B. de Bruin, *Eur. J. Inorg. Chem.* **2012**, 340; e) W. Kaim, *Eur. J. Inorg. Chem.* **2012**, 343.

[2] a) R. H. Crabtree, *New J. Chem.* **2011**, *35*, 18; b) W. I. Dzik, J. I. van der Vlugt, J. N. H. Reek, B. de Bruin, *Angew. Chem. Int. Ed.* **2011**, *50*, 3356; c) V. Lyaskovskyy, B. de Bruin, *ACS Catal.* **2012**, *2*, 270; d) O. R. Luca, R. H. Crabtree, *Chem. Soc. Rev.* **2013**, *42*, 1440; e) V. Blanco, D. A. Leigh, V. Marcos, *Chem. Soc. Rev.* **2015**, *44*, 5341; f) S. M. Guillaume, E. Kirillov, Y. Sarazin, J.-F. Carpentier, *Chem. Eur. J.* **2015**, *21*, 7988.

[3] a) U. Siemeling, *Z. Anorg. Allg. Chem.* **2005**, *631*, 2957; b) Z. Liu, *Science* **2003**, *302*, 1543; c) J. W. Sibert, P. B. Forshee, V. Lynch, *Inorg. Chem.* **2005**, *44*, 8602; d) H. Wang, D. Qi, Z. Xie, W. Cao, K. Wang, H. Shang, J. Jiang, *Chem. Commun.* **2013**, *49*, 889; e) K. Green, N Gauthier, H. Sahnoune, G Argouarch, L. Toupet, K. Costuas, A. Bondon, B. Fabre, J.-F. Halet, F. Paul, *Organometallics* **2013**, *32*, 4366.

[4] Another approach uses ferrocenyl substituents as oxidisable entities to modify the solubility of a complex. Plenio and co-workers have demonstrated in a seminal paper that the activity of Fc-decorated Grubbs-Hoveyda catalysts can be switched by one-electron oxidation/reduction. Loss of activity is attributed to the low solubility of the cationic complex catalyst: M. Süßner, H. Plenio, *Angew. Chem.* **2005**, *117*, 7045, *Angew. Chem. Int. Ed.* **2005**, *44*, 6885; see also b) C. A. Fleckenstein, H. Plenio, *Adv. Synth. Catal.* **2006**, *348*, 1058.

[5] For a recent study on the effect of a ferrocene moiety as redox active site, see: S. Kuriyama, K. Arashiba, K. Nakajima, H. Tanaka, K. Yoshizawa, Y. Nishibayashi, *Chem. Sci.* **2015**, *6*, 3940.

[6] Metalloligands have been used to prepare multimetallic complexes. See *e.g.*: a) T. T. Nadasdi, D. W. Stephan, *Organometallics* **1992**, *11*, 116; b) T. Sue, Y. Sunada, H. Nagashima, *Eur. J. Inorg. Chem.* **2007**, 2897; c) D. L. Reger, J. R. Gardinier, S. Bakbak, R. F. Semeniuc, U. H. F. Bunz, M. D. Smith, *New J. Chem.* **2005**, *29*, 1035; d) T. Matsumoto, M. Wakizaka, H. Yano, A. Kobayashi, H.-C. Chang, M. Kato, *Dalton Trans.* **2012**, *41*, 8303; e) M.-G. Alexandru, D. Visinescu, A. M. Madalan, F. Lloret, M. Julve, M. Andruh, *Inorg. Chem.* **2012**, *51*, 4906. For several applications in MOF chemistry see *e.g.*: f) S. R. Halper, L. Do, J. R. Stork, S. M. Cohen, *J. Am. Chem. Soc.* **2006**, *128*, 15255; g) S. Kitagawa, R. Kitaura, S. Noro, *Angew. Chem. Int. Ed.* **2004**, *43*, 2334; general review: h) G. Kumar, R. Gupta, *Chem. Soc. Rev.* **2013**, *42*, 9403.

[7] Selected examples of metallocene-based ligand scaffolds containing phosphine donors with a strong focus on redox-switchable catalysis (RSC): a) I. M. Lorkovic, R. R. Duff, M. S. Wrighton, *J. Am. Chem. Soc.* **1995**, *117*, 3617; b) R. T. Hembre, J. S. McQueen, V. W. Day, *J. Am. Chem. Soc.* **1996**, *118*, 798; c) P. Neumann, H. Dib, A.-M. Caminade, E. Hey-Hawkins, *Angew. Chem.* **2015**, *127*, 316; d) M. Chen, B. Yang, C. Chen, *Angew. Chem. Int. Ed.* **2015**, *54*, 15520.

[8] Selected examples of metallocene-based ligand scaffolds containing nitrogen donors with a strong focus on redox-switchable catalysis (RSC): a) C. K. A. Gregson, V. C. Gibson, N. J. Long, E. L. Marshall, P. J. Oxford, A. J. P. White, *J. Am. Chem. Soc.* **2006**, *128*, 7410; b) E. M. Broderick, N. Guo, T. Wu, C. S. Vogel, C. Xu, J. Sutter, J. T. Miller, K. Meyer, T. Cantat, P. L. Diaconescu, *Chem. Commun.* **2011**, *47*, 9897; c) E. M. Broderick, N. Guo, C. S. Vogel, C. Xu, J. Sutter, J. T. Miller, K. Meyer, P. Mehrkhodavandi, P. L. Diaconescu, *J. Am. Chem. Soc.* **2011**, *133*, 9278; d) X. Wang, A. Thevenon, J. L. Brosmer, I. Yu, S. I. Khan, P. Mehrkhodavandi, P. L. Diaconescu, *J. Am. Chem. Soc.* **2014**, *136*, 11264

[9] Selected reviews: a) A. J. Arduengo, *Acc. Chem. Res.* **1999**, *32*, 913; b) D. Bourissou, O. Guerret, F. P. Gabbaï, G. Bertrand, *Chem. Rev.* **2000**, *100*, 39; c) W. A. Herrmann, *Angew. Chem. Int. Ed.* **2002**, *41*, 1290; d) F. E. Hahn, M. C. Jahnke, *Angew. Chem. Int. Ed.* **2008**, *47*, 3122; e) J. Vignolle, X. Cattoën, Didier Bourissou, *Chem. Rev.* **2009**, *109*, 3333; f) P. de Frémont, N. Marion, S. P. Nolan, *Coord. Chem. Rev.* **2009**, *253*, 862; g) K. Öfele, E. Tosch, C. Taubmann, W. A. Herrmann, *Chem. Rev.* **2009**, *109*, 3408; h) L. Mercs, M. Albrecht, *Chem. Soc. Rev.* **2010**, *39*, 1903; i) T. Dröge, F. Glorius, *Angew. Chem. Int. Ed.* **2010**, *49*, 6940; j) *N-Heterocyclic Carbenes−Effective Tools for Organometallic Synthesis*; S. P. Nolan (Ed.); Wiley−VCH Weinheim, Germany, **2014**; k) M. N. Hopkinson, C. Richter, M. Schedler, F. Glorius, *Nature* **2014**, *510*, 485.

[10] Selected reviews on singlet carbenes derived from ferrocene and closely related sandwich complexes: a) B. Bildstein, *J. Organomet. Chem.* **2001**, *617-618*, 28; b) U. Siemeling, *Eur. J. Inorg. Chem.* **2012**, 3523.

[11] Studies on diaminocarbene[3]ferrocenophanes and closely related Fc-decorated NHC ligands and their complexes: a) D. M. Khramov, E. L. Rosen, V. M. Lynch, C. W. Bielawski, *Angew. Chem.* **2008**, *120*, 2299; b) U. Siemeling, C. Färber, C. Bruhn, *Chem. Commun.* **2009**, 98; c) U. Siemeling, C. Färber, M. Leibold, C. Bruhn, P. Mücke, R. F. Winter, B. Sarkar, M. von Hopffgarten, G. Frenking, *Eur. J. Inorg. Chem.* **2009**,

4607; d) E. L. Rosen, C. D. Varnado Jr., A. G. Tennyson, D. M. Khramov, J. W. Kamplain, D. H. Sung, P. T. Cresswell, V. M. Lynch, C. W. Bielawski, *Organometallics* **2009**, *28*, 6695; e) C. D. Varnado, V. M. Lynch, C. W. Bielawski, *Dalton Trans.* **2009**, 7253; f) K. Arumugam, J. Chang, V. M. Lynch, C. W. Bielawski, *Organometallics* **2013**, *32*, 4334; j) U. Siemeling, C. Färber, C. Bruhn, S. Fürmeier, T. Schulz, M. Kurlemann, S. Tripp, *Eur. J. Inorg. Chem.* **2012**, 1413; k) C. D. Varnado Jr, E. L. Rosen, M. S. Collins, V. M. Lynch, C. W. Bielawski, *Dalton Trans.* **2013**, *42*, 13251; l) K. Arumugam, J. Chang, V. M. Lynch, C. W. Bielawski, *Organometallics* **2013**, *32*, 4334; m) A. R. Petrov, A. Derheim, J. Oetzel, M. Leibold, C. Bruhn, S. Scheerer, S. Oßwald, R. F. Winter, U. Siemeling, *Inorg. Chem.* **2015**, *54*, 6657; n) U. Siemeling, C. Färber, C. Bruhn, M. Leibold, D. Selent, W. Baumann, M. von Hopffgarten, C. Goedecke, G. Frenking, *Chem. Sci.* **2010**, *1*, 697; o) S. Rittinghaus, C. Färber, C. Bruhn, U. Siemeling, *Dalton Trans.* **2014**, *43*, 3058.

[12] a) A. J. Arduengo, D. Tapu, W. J. Marshall, *Angew. Chem. Int. Ed.* **2005**, *44*, 7240; b) A. J. Arduengo, D. Tapu, W. J. Marshall, *J. Am. Chem. Soc.* **2005**, *127*, 16400.

[13] a) B. Hildebrandt, W. Frank, C. Ganter, *Organometallics* **2011**, *30*, 3483; b) B. Hildebrandt, S. Raub, W. Frank, C. Ganter, *Chem. Eur. J.* **2012**, *18*, 6670.

[14] a) L. Hettmanczyk, S. Manck, C. Hoyer, S. Hohloch, B. Sarkar, *Chem. Commun.* **2015**, *51*, 10949; b) S. Ibáñez, M. Poyatos, L. N. Dawe, D. Gusev, E. Peris, *Organometallics* **2016**, *35*, 2747; c) K. Arumugam, C. D. Varnado, Jr., S. Sproules, V. M. Lynch, C. W. Bielawski, *Chem. Eur. J.* **2013**, *19*, 10866.

[15] I. Kuzu, I. Krummenacher, J. Meyer, F. Armbruster, F. Breher, *Dalton Trans.* **2008**, 5836.

[16] Selected examples: a) F. Breher, J. Grunenberg, S. Lawrence, P. Mountford, H. Rüegger, *Angew. Chem. Int. Ed.* **2004**, *43*, 2521; b) I. Krummenacher, H. Rüegger, F. Breher, *Dalton Trans.* **2006**, 1073; c) H. R. Bigmore, J. Meyer, I. Krummenacher, H. Rüegger, E. Clot, P. Mountford, F. Breher, *Chem. Eur. J.* **2008**, *14*, 5918; d) I. Kuzu, I. Krummenacher, I. J. Hewitt, Y. Lan, V. Mereacre, A. K. Powell, P. Höfer, J. Harmer, F. Breher, *Chem. Eur. J.* **2009**, *15*, 4350; e) I. Fernández, P. Oña-Burgos, F. Armbruster, I. Krummenacher, F. Breher, *Chem. Commun.* **2009**, 2586; f) M. G. Cushion, J. Meyer, A. Heath, A. D. Schwarz, I. Fernández, F. Breher, P. Mountford, *Organometallics* **2010**, *29*, 1174; g) D. Kratzert, D. Leusser, D. Stern, J. Meyer, F. Breher, D. Stalke, *Chem. Commun.* **2011**, *47*, 2931; h) J. Meyer, I. Kuzu, S. González-Gallardo, F. Breher, *Z. Anorg. Allg. Chem.* **2013**, *639*, 301; i) J. Meyer, S. González-Gallardo, S. Hohnstein, D. Garnier, M. K. Armbruster, K. Fink, W. Klopper, F. Breher, *Chem. Eur. J.* **2015**, *21*, 2905; j) I. Trapp, S. González-Gallardo, S. Hohnstein, D. Garnier, P. Oña-Burgos, F. Breher, *Dalton Trans.* **2014**, *43*, 4313; k) I. Kuzu, A. Baldes, F. Weigend, F. Breher, *Polyhedron* **2016**, in press (http://dx.doi.org/10.1016/j.poly.2016.09.017).

[17] a) S. González-Gallardo, I. Kuzu, P. Ona-Burgos, T. Wolfer, C. Wang, K. W. Klinkhammer, W. Klopper, S. Bräse, F. Breher, *Organometallics* **2014**, *33*, 941.

[18] S. Styra, S. González-Gallardo, F. Armbruster, P. Oña-Burgos, E. Moos, M. Vonderach, P. Weis, O. Hampe, A. Grün, Y. Schmitt, M. Gerhards, F. Menges, M. Gaffga, G. Niedner-Schatteburg, F. Breher, *Chem. Eur. J.* **2013**, *19*, 8436.

[19] a) C. A. Tolman, *Chem. Rev.* **1977**, *77*, 313; b) S. Wolf, H. Plenio, *J. Organomet. Chem.* **2009**, *694*, 1487; c) R. A. Kelly III, H. Clavier, S. Giudice, N. M. Scott, E. D. Stevens, J. Bordner, I. Samardjiev, C. D. Hoff, L. Cavallo, S. P. Nolan, *Organometallics* **2008**, *27*, 202; d) D. J. Nelson, S. P. Nolan, *Chem. Soc. Rev.* **2013**, *42*, 6723.

[20] As summarized in ref. [11d], „the redox tunability of these ligands does not strongly depend on the specific chemical identity of the redox-active functional group. Rather, the overall charge imparted to the molecule upon redox changes appears to be the origin of the ligand's attenuated donating ability."

[21] T. M. Miller, K. J. Ahmed, M. S. Wrighton, *Inorg. Chem.* **1989**, *28*, 2347.

[22] a) F. Breher, H. Rüegger, *Angew. Chem.* **2005**, *117*, 477; *Angew. Chem. Int. Ed.* **2005**, *44*, 473; b) I. Krummenacher, F. Breher, *Z. Anorg. Allg. Chem.* **2006**, *632*, 965; c) I. Krummenacher, C. Oschwald, H. Rüegger, F. Breher, *Z. Anorg. Allg. Chem.* **2007**, *633*, 2354; d) I. Krummenacher, I. Fernández, H. Rüegger, F. Weigend, F. Breher, *Dalton Trans.* **2009**, 5335; e) F. Armbruster, I. Fernández, F. Breher, *Dalton Trans.* **2009**, 5612; f) F. Armbruster, T. Augenstein, P. Oña-Burgos, F. Breher, *Chem. Eur. J.* **2013**, 19, 17899; g) T. Augenstein, F. Dorner, K. Reiter, H. E. Wagner, D. Garnier, W. Klopper, F. Breher, *Chem. Eur. J.* **2016**, *22*, 7935; h) M. Zimmer, F. Rupp, P. Singer, F. Walz, F. Breher, W. Klopper, R. Diller, M. Gerhards, *Phys. Chem. Chem. Phys.* **2015**, *17*, 14138; i) Y. Schmitt, K. Chevalier, F. Rupp, M. Becherer, A. Grün, A. M. Rijs, F. Walz, F. Breher, R. Diller, M. Gerhards, W. Klopper, *Phys. Chem. Chem. Phys.* **2014**, *16*, 8332; j) F. Armbruster, J. Meyer, A. Baldes, P. Oña-Burgos, I. Fernández, F. Breher, *Chem. Commun.* **2011**, *47*, 221; k) D. Nied, E. Matern, H. Berberich, M. Neumaier, F. Breher, *Organometallics* **2010**, *29*, 6028.

[23] M. Kaupp, *J. Comput. Chem.* **2006**, *28*, 320.

[24] Selected reviews: a) W. Petz, *Chem. Rev.* **1986**, *86*, 1019; b) M. F. Lappert, R. S. Rowe, *Coord. Chem. Rev.* **1990**, *100*, 267; c) O. Kühl, *Coord. Chem. Rev.* **2004**, *248*, 411; d) S. Nagendran, H. W. Roesky, *Organometallics* **2008**, *27*, 457; e) M. Asay, C. Jones, M. Driess, *Chem. Rev.* **2011**, *111*, 354; f) J. Barrau, G. Rima, *Coord. Chem. Rev.* **1998**, *178-180*, 593; g) N. Tokitho, R. Okazaki, *Coord. Chem. Rev.* **2000**, *210*, 251; h) M. F. Lappert, *Main Group Metal Chem.* **1994**, *17*, 183; i) W.-P. Leung, K.-W. Kan, K.-H. Chong, *Coord. Chem. Rev.* **2007**, *251*, 2253; j) L. Álvarez-Rodríguez, J. A Cabeza, P. García-Álvarez, D. Polo, *Coord. Chem. Rev.* **2015**, *300*, 1; k) A. V. Zabula, F. E. Hahn, *Eur. J. Inorg. Chem.* **2008**, 5165; l) J. Baumgartner, C. Marschner, *Rev. Inorg. Chem.* **2014**, *34*, 119. Pioneering papers in the area of NHGe: m) Ref [32]; n) Ref. [35h]. For attempts of Wrackmeyer and co-workers to prepare the Fc-based NHSn, see: o) B. Wrackmeyer, E. V. Klimkina, W. Milius, *Z. Anorg. Allg. Chem.* **2006**, *632*, 2331; p) B. Wrackmeyer, W. Milius, H. E. Maisel, H. Vollrath, M. Herberhold, *Z. Anorg. Allg. Chem.* **2003**, *629*, 1169. For a successfull synthesis, see q) ref. [27].

[25] W. Wang, S. Inoue, S. Enthaler, M. Driess, *Angew. Chem.* **2012**, *124*, 6271; *Angew. Chem. Int. Ed.* **2012**, *51*, 6167.

[26] a) Florian Walz, Dissertation, Karlsruher Institut für Technologie (KIT), September 2015 (ISBN 978-3-8325-4208-5); b) Jan Oetzel, Dissertation, Universität Kassel, September 2015.

[27] J. Oetzel, N. Weyer, C. Bruhn, M. Leibold, B. Gerke, R. Pöttgen, M. Maier, R. F. Winter, M. C. Holthausen, U. Siemeling, *Chem. Eur. J.* submitted.

[28] See, e.g. a) R. M. Haak, S. J. Wezenberg, A. W. Kleij, *Chem. Commun.* **2010**, *46*, 2713; b) J. I. van der Vlugt, *Eur. J. Inorg. Chem.* **2012**, 363; c) J. Park, S. Hong, *Chem. Soc. Rev.* **2012**, *41*, 6931; d) I. Bratko, M. Gómez, *Dalton Trans.* **2013**, *42*, 10664.

[29] For a recent study on differential many-body cooperativity in electronic spectra of oligonuclear transition-metal complexes, see J. Chmela, M. E. Harding, D. Matioszek, C. E. Anson, F. Breher, W. Klopper, *Chem. Phys. Chem.* **2016**, *17*, 37.

[30] a) A. Shafir, M. P. Power, G. D. Whitener, J. Arnold, *Organometallics* **2000**, *19*, 3978; b) A. R. Petrov, K. Jess, M. Freytag, P. G. Jones, M. Tamm, *Organometallics* **2013**, *32*, 5946; c) M. A. Abdulmalic, T. Rüffer, *Bull. Chem. Soc. Jpn.* **2013**, *86*, 724.

[31] a) A. Shafir, J. Arnold, *Inorg. Chim. Acta* **2003**, *345*, 216; b) J. A. Lee, B. N. Williams, K. R. Ogilby, K. L. Miller, P. L. Diaconescu, *J. Organomet. Chem.* **2011**, *696*, 4090; c) U. Siemeling, T.-C. Auch, O. Kuhnert, M. Malaun, H. Kopacka, B. Bildstein, *Z. Anorg. Allg. Chem.* **2003**, *629*, 1334.

[32] a) J. D. Cotton, C. S. Cundy, D. H. Harris, A. Hudson, M. F. Lappert, P. W. Lednor, *J. Chem. Soc., Chem. Commun.* **1974**, 651; b) D. H. Harris, M. F. Lappert, *J. Chem. Soc., Chem. Comm.* **1974**, 895.

[33] D. R. Scott, R. S. Becker, *J. Organomet. Chem.* **1965**, *4*, 409.

[34] S. Duhović, P. L. Diaconescu, *Polyhedron* **2013**, *52*, 377.

[35] Selected examples: a) W. A. Herrmann, M. Denk, J. Behm, W. Scherer, F.-R. Klingan, H. Bock, B. Solouki, M. Wagner, *Angew. Chem. Int. Ed. Engl.* **1992**, *31*, 1485; b) P. Bazinet, G. P. A. Yap, D. S. Richeson, *J. Am. Chem. Soc.* **2001**, *123*, 11162; c) S. Krupski, R. Pöttgen, I. Schellenberg, F. E. Hahn, *Dalton Trans.* **2014**, *43*, 173; d) J. Pfeiffer, W. Maringgele, M. Noltemeyer, A. Meller, *Chem. Ber.* **1989**, *122*, 245; e) O. Kühl, P. Lönnecke, J. Heinicke, *Polyhedron* **2001**, *20*, 2215; f) S. Krupski, J. V. Dickschat, A. Hepp, T. Pape, F. E. Hahn, *Organometallics*, **2012**, *31*, 2078; g) F. E. Hahn, A. V. Zabula, T. Pape, A. Hepp, *Z. Anorg. Allg. Chem.* **2008**, *634*, 2397; h) M. Veith, M. Grosser, *Z. Naturforsch.* **1982**, *37b*, 1375; h) P. Bazinet, G. P. A. Yap, D. S. Richeson, *J. Am. Chem. Soc.* **2001**, *123*, 11162; i) M. Stender, A. D. Phillips, P. P. Power, *Inorg.*

10.1002/chem.201605073

Chem. **2001**, *40*, 5314; j) M. Driess, S. Yao, M. Brym, C. van Wüllen, *Angew. Chem.* **2006**, *118*, 4455; *Angew. Chem., Int. Ed.* **2006**, *45*, 4349; k) S. Krupski, C. Schulte to Brinke, H. Koppetz, A. Hepp, F. E. Hahn, *Organometallics*, **2015**, *34*, 2624.

[36] Selected exampes: a) M. Driess, S. Yao, M. Brym, C. Van Wüllen, D. Lentz, *J. Am. Chem. Soc.* **2006**, *128*, 9628; b) H. V. R. Dias, Z. Wang, W. Jin, *Coord. Chem. Rev.* **1998**, *176*, 67; c) B. Gehrhus, M. F. Lappert, *J. Organomet. Chem.* **2001**, *617-618*, 209; d) Y. Ding, H. W. Roesky, M. Noltemeyer, H.-G. Schmidt, P. P. Power, *Organometallics* **2001**, *20*, 1190; e) A. E. Ayers, T. M. Klapötke, H. V. R. Dias, *Inorg. Chem.* **2001**, *40*, 1000; for a related four-membered germylene, see e.g. f) M. Veith, R. Lisowski, *Angew. Chem.* **1988**, *100*, 1124; *Angew. Chem., Int. Ed. Engl.* **1988**, *27*, 1087

[37] a) A. Poater, B. Cosenza, A. Correa, S. Giudice, F. Ragone, V. Scarano, L. Cavallo, *Eur. J. Inorg. Chem.* **2009**, 1759; b) https://www.molnac.unisa.it/OMtools/sambvca.php.

[38] Note that we had to substitute Ge for Si in the calculation of the %V_{bur} value because Ge is not available in the sambvca database.[37b] However, since germanium and silicon are very similar in size, we expect only slight deviations from the „true“ value for **4**.

[39] a) Ref. [3]; b) H. Clavier, S. P. Nolan, *Chem. Commun.* **2010**, *46*, 841; c) O. Diebolt, G. C. Fortman, H. Clavier, A. M. Z. Slawin, E. C. Escudero-Adán, J. Benet-Buchholz, S. P. Nolan, *Organometallics* **2011**, *30*, 1668; d) N. Fey, M. F. Haddow, J. N. Harvey, C. L. McMullin, A. G. Orpen, *Dalton Trans.* **2009**, 8183.

[40] a) K. Hinkelmann, J. Heinze, H.-T. Schacht, J. S. Field, H. Vahrenkamp, *J. Am. Chem. Soc.* **1989**, *111*, 5078; b) J. Heinze, *Angew. Chem.* **1984**, *96*, 823; *Angew. Chem. Int. Ed.* **1984**, *23*, 831.

[41] $E^p{}_a$ values of 0.84 and 1.20 V *vs.* Ag/AgCl (THF/[Bu$_4$N][ClO$_4$]) have been reported for unsaturated and saturated germylenes (CHN*t*Bu)$_2$Ge and (CH$_2$N*t*Bu)$_2$Ge, respectively, which corresponds to $E^p{}_a \cong 0.48$ and 0.85 V vs. Fc/Fc$^+$. Interestingly, (CHN*t*Bu)$_2$Ge gave a reversible redox process centred at $E^0{}_{1/2}$ = 0.41 V *vs.* Ag/AgCl in 1,2-DCB using [Bu$_4$N][ClO$_4$] as electrolyte, *i.e. ca.* 0.06 V vs. Fc/Fc$^+$. A. Dhiman, T. Müller, R. West, J. Y. Becker, *Organometallics* **2004**, *23*, 5689.

[42] F. Basolo, R. G. Pearson, *Progr. Inorg. Chem.* **1962**, *4*, 381.

[43] See, *e.g.*: a) O. Kühl, P. Lönnecke, J. Heinicke, *Inorg. Chem.* **2003**, *42*, 2836; b) D. Matioszek, N. Katir, N. Saffon, A. Castel, *Organometallics* **2010**, *29*, 3039; c) I. Saur, S. Garcia Alonso, H. Gornitzka, V. Lemierre, A. Chrostowska, J. Barrau, *Organometallics* **2005**, *24*, 2988.

[44] a) F. Ullah, O. Kühl, G. Bajor, T. Veszprémi, P. G. Jones, J. Heinicke, *Eur. J. Inorg. Chem.* **2009**, 221; b) F. Ullah, G. Bajor, T. Veszprémi, P. G. Jones, J. Heinicke, *Angew. Chem.* **2007**, *119*, 2751; *Angew. Chem. Int. Ed.* **2007**, *46*, 2697; c) A. V. Zabula, F. E. Hahn, T. Pape, A. Hepp, *Organometallics* **2007**, *26*, 1972.

[45] Typically, the metal-to-metal communication is assessed by electrochemical experiments. For a nice review article on the triumphs and defeats of half-wave potential splittings $\Delta E_{1/2}$ as a measure of electronic coupling in mixed-valent systems, see: R. Winter, *Organometallics* **2014**, *33*, 4517.

[46] Small deviations of the HOMO energy levels have to be expected due to the different tilting of the Cp rings in the model compounds: J. C. Green, *Chem. Soc. Rev.* **1998**, *27*, 263.

[47] In order to compare calculated harmonic frequencies with experimental values the computed vibrational frequencies have to be scaled. A typical empirical factor for the chosen theoretical method is 0.9671 (B3LYP/def2-TZVP): M. K. Kesharwani, B. Brauer, J. M. L. Martin, *J. Phys. Chem. A* **2015**, *119*, 1701.

[48] W. A. Herrmann, J. Schütz, G. D. Frey, E. Herdtweck, *Organometallics* **2006**, *25*, 2437.

[49] For the TEP calculations, we have consistently used the equations given in ref. [19b] and [19c].

[50] Germylenes are usually categorized among the weak σ-donor and good π-acceptor ligands. See Ref. [24] and O. Kühl, K. Lifson, W. Langel, *Eur. J. Org. Chem.* **2006**, 2336.

[51] We refrain from giving any dicimal places and quote rounded values.

[52] a) M. W. Löble, P. Oña-Burgos, I. Fernández, C. Apostolidis, A. Morgenstern, O. Walter, F. Bruchertseifer, P. Kaden, T. Vitova, J. Rothe, K. Dardenne, N. L. Banik, A. Geist, M. A. Denecke, F. Breher, *Chem. Sci.* **2013**, *4*, 3717; b) M. Casimiro, P. Oña-Burgos, J. Meyer, S. Styra, I. Kuzu, F. Breher, I. Fernández, *Chem. Eur. J.* **2013**, *19*, 691; c) DiffAtOnce Molecular Diffusion, available at www.diffatonce.com.

[53] *TURBOMOLE, V6.0, 2009*; a development of University of Karlsruhe (TH) and Forschungszentrum Karlsruhe GmbH 1989-2007: TURBOMOLE GmbH, since 2007, available from http://www.turbomole.com.

[54] a) C. Lee, W. Yang, R. G. Parr, *Phys. Rev. B* **1988**, *37*, 785; b) A. D. Becke, *J. Chem. Phys.* **1993**, *98*, 5648.

[55] F. Weigend, R. Ahlrichs, *Phys. Chem. Chem. Phys.* **2005**, *7*, 3297.

[56] G. M. Sheldrick, *Acta Cryst.* **2015**, *A71*, 3.

[57] G. M. Sheldrick, *Acta Cryst.* **2015**, *C71*, 3.

[58] A. L. Spek, *Acta Cryst.*, **2015**, *C71*, 9.

Entry for the Table of Contents:

FULL PAPER

The redox-switchable germylene [Fc(NMes)$_2$Ge] based on a [3]ferrocenophane ligand arrangement, alongside some transition metal complexes, are reported. The change in the ligating properties upon oxidation were elucidated by DFT calculations on neutral and cationic bimetallic model complexes.

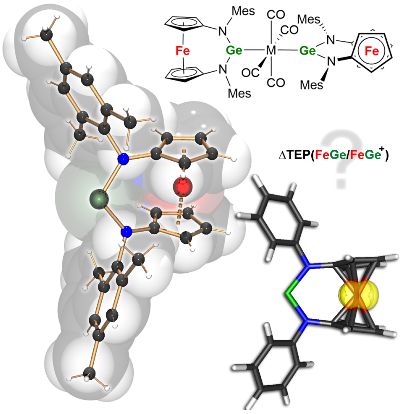

*Florian Walz, Eric Moos, Delphine Garnier, Ralf Köppe, Christopher E. Anson, Frank Breher**

1 – 13

A Redox-Switchable Germylene and its Ligating Properties in Selected Transition Metal Complexes